World Journal of Engineering Research and Technology
WJERT
www.wjert.org
Impact Factor Value: 5.924

CHS COLD FORM STEEL MEMBERS STRENGTHENED WITH BIDIRECTIONAL FRP SHEET

Eng. Faisal Alharbi*[1] and Dr. Alaa Almosawe[2]

[1]A Professional Engineer in the Ministry of Transport in Saudi Arabia.

[2]Faculty of Science, Engineering and Technology Swinburne University of Technology.

Article Received on 05/11/2020 **Article Revised on 25/11/2020** **Article Accepted on 15/12/2020**

***Corresponding Author**
Eng. Faisal Alharbi
A professional engineer in the Ministry of Transport in Saudi Arabia.

ABSTRACT

The main purpose of this research paper experimental analysis is conducted with the aim of establishing the static load of the lateral loads on the structures in line with the fiber-reinforced polymer or FRP to strengthen the CHS of the steel members. The norm encompasses the evaluation of the transverse static load which the structures are likely to face in the situations when they are subjected to the loading at the decisive mid-spans. There are gathering of the information from the various literature reviews as well as the appraisal of the journals in line with the static load and the effects which the fiber-reinforced polymer or FRP to strengthen the CHS of the steel members have on the structures in the long run. There were 4 Groups of CHS which wrapped via CFRP under libation condition. It has been achieved the main objective of the research to Strengthen CHS member via CFER. The evaluation also incorporates the utilization of the 13 medium-scale specimens which Ares used in the investigation of the FRP on the Circular hollow structures. However, the experiment includes the application of both the glass-fiber-reinforced polymer and the carbon-fiber-reinforced polymer which were applied in the process as the strengthening materials. There was remarkable static load in line with the resistance capacity and this was recorded by the externally and bonded CFRP sheet. It vividly indicated the reduction in the lateral displacement with a tune of at least 10.5% as compared to the bare specimen (Grouo#2). Furthermore, the group# 2 which rise up strength until 17.74%. On other the hand, it is possible for us to compare Group#1 with Group#2 which achieved 42.22% for Group#1.

Finally, this paper simulated multi cases of CHS as lathing and sand plaster surface. The most resulting indication that there is many of benefit to using CFRP to a stronger member of the structure. This reported result of much time which has been spender in Lab at Swinburne University during 12 Weeks. This period study Considered very short to exams many of CHS and CFRP with different layers but I will complete tests in Ph.D. in future near.

I. CHAPTER ONE

II. INTRODUCTION

Description of CHS Steel

Over the past years, there has been increase in the application of the CHS cold-formed steel. However, the hollow structural sections mainly defined as the metal profile type which has the hollow cross-section. The term has continued to gain momentums and predominantly use in the United States of America as well as the related countries which applies the US engineering and construction terminology. The hollow structural steel members in most cases tend to have the square, circular as well as rectangular sections however; there are situations under which the HSS can also have the elliptical shapes. Notably, the HSS defined as the composition of the structural steel as per the related codes (Li et al. 2012).

On the other hand, the circular hollow section also describes as the parametric round steel tubes have gained advance application in the variety of construction industries across the board. The steel sections used in the CHS mainly rolled from either the slit coil or the steel sheets. Preferably, the slit strip employs the sizing section and the formation type of the steel which involve the normal cold forming of the steel from the mills. The milling process incorporates various phases which the CHS has to undergo. As the sheet passes gradually over the phases, the steel sheet tends to bend and start to change the radii on every stage. The process continues until the ends of the steels often pressed together and thereby welded inline. Furthermore, the circular steel sections often rolled from different materials. The most commonly used materials in the process include the cold and the hot rolled steel tubes. Notably, the major application of the hot rolled sections is essentially utilized for the structural purposes. On the other hand, the cold rolled tubes have the high ability as far as the bending is considered and thus, used to give the aesthetic appearance once the powder coat is applied (Islam et al., 2012).

Furthermore, there are instances under which the steel sections can either be internally scarfed or fin controlled. Preferably, the fin controlled steel sections means that the overall internal weld section bead has decisively been meticulous to nearly absolute minimum. On the other hand, the scarfed steel tube refers to the one which the inline have been by the weld bead. The norm helps in ensuring that the tubes are often suitable to be used in the mandrel bending. Also, the drawn steel sections have continued to played fundamental roles in the building and steel industry. There are possibilities of drawing the steel sections from the makeable available standards and sized tubes. The application of the various precisions ensures that the inner diameters of the parametric steel tube are often controlled via the application of the mandrel. On the other hand, the outer diameters sophisticated drawn down over and done with a die (Wu et al. 2012).

When the structural forms are sophisticated subjected to the load impacts, and then there are possibilities of the elements to experience the viable premature and local buckling. The norm is common in the steel components such as the amicable circular tubular sections. Thus, the application of the high-strength and advanced composites materials often helps in accompanying the structural minimal weight. Essence, there is the need of the composite materials to accompany in ensuring that there is structural minimal weight have led to evaluation of the effectiveness of the supplementary external in the reinforcing materials (Al- saad et al., 2018).

Various Fiber-Reinforced Polymers (FRP)

On the other hand, the application of the fibre-reinforced polymers (FRP) as well as the steel tends to exhibit different range of phenomena and thus, is highly encouraged in the process. The norms in the most cases are intertwined with the thin-bonded carbon FRP (CFRP) sheets.

The incorporation of the elements aims at ensuring that there not only the marked bearing but also the connotations which indicates on how the various materials should be designed.

Economic Viability

There many examples which have demonstrated the overall excellent circular hollow section properties as far as the structural element is concerned. The excellent properties mainly exhibited in the norms such as the tension, resisting compression, torsion and

bending. Furthermore, various analogies have depicted that the circular hollow section exhibits decisive traits which have given the sections best shapes when the overall elements are subjected to innumerable impacts. The circular hollow section in most cases many be subjected to the wave, wind, water as well as dead loads. However, the circular hollow section in most occasions tends to utilize the characteristics and combines them with the architecturally attractive shape. Notably, the circular hollow section structures have smaller surface area as compared to the similar edifices with the open sections. The norm in correlation with the absence of the amicable sharp corners often results to more corrosion protection. Thus, the considerations under this situation have resulted to the need to have excellent properties which often than not will aim at designing structures with light and open designs. The designs should also incorporate the simple joints. The joints should be worked in a manner that they have the ability to eliminate both the stiffening and the gussets. Moreover, joint strength forms the fundamental influence aspect in the design and thus, it must be consider at all cost. In fact, the geometric properties influence the joint strengths decisively (Chen et al., 2018). Thus, it is important for the designers to understand the overall behaviors associated with the optimum designs and takes them into consideration when developing the conceptual designs. Furthermore, most evaluations have established that the cost of the hollow section materials is habitually higher as compared to the ones for the open sections. However, these costs can be lower when one embarks on using the low weights in construction, applying small paint for the makeable corrosion protection as well as reducing the fabrication costs by using the simple joints. Moreover, many of the applications in which the circular hollow sections are utilized, indicates that the material is economically compete with the spectra of the open design. The incorporation of the circular hollow section with the fibre-reinforced polymers (FRP) should highly be encouraged (Wang et al., 2018).

III. CHAPTER TWO

IV. LITERATURE REVIEW

Introduction

This section encompasses on the evaluation of the literature Review utilized in this research work. Different sources mainly appraised in line with the research topic and various conclusions drawn as indicated in the various sections below (Shen et al., 2018).

Circular hollow-section strengthen cylindrical

In recent times, there have been increases of the structural failures under blast loading, influenced by rising numbers of terrorist attacks as well as increasing of traffics on the roads in all parts of the world. Circular hollow-section strengthened cylindrical associates are very attractive preferences to use as a structural columns and also on other structural apparatuses such as horizontal associates in road barriers, beams, jacket legs, utility transmission towers, braces of offshores as well as artistic purposes in which the axial stationary forces are very low and insignificant (Chen et al., 2018). Transverse influence forces are highly expected on the mentioned members from vessels impacts or vehicles, lying debris and from terrorist attacks. Therefore, if they are not properly designed for repelling such transverse impact loading, the existing tubular members are highly vulnerable to these transverse impacts as experienced and reported in different parts of the world (Tafsirojjaman et al., 2019).

There is need for stronger structures to be put in place to avoid high risk of structural failures across the world. When metallic members are strengthened using extra metal plates through welding to obtain these stronger structures, it is likely to be time-consuming events, at the same time it can result into the rising of dead load of the already existing structures. In addition to these, strengthening of metallic associates will instead increase the risk of steel deterioration as a result of corrosion experienced in unfriendly environmental conditions. Because of these fore mentioned problems, alternative sustainable and suitable strengthening techniques for the purposes of avoiding all these difficulties needed to be brought forward so that it minimizes both human casualties and structural damages influenced by different dynamic event (Shen et al.,2019).In the modern times worldwide, there is an acceptable alternative strengthening technique by all the structural engineers across the world due to its unlimited advantages as shown by the studies. This alternative strengthening method is known as fibre-reinforced polymer (FRP) and its advantages are; fast constructions accompany by minimum interruption of services, high strength-to- weight ratio, as well as highly resistance to corrosions (Kadhim et al., 2019).

Fiber-reinforced polymer strengthening of steel

In modern days, fiber-reinforced polymer strengthening of steel members has received major attention in relation to innovative composites buildings. In order to overcome the

main problems related to conventional strengthening methods of the metallic structures. According to (Fu et al., 2016) research studies indicated that there various aspects undertaken so as to comprehend the joint performance of carbon-fibre-reinforced polymer reinforced steel plates. Even though fibre-reinforced polymer composites as well as the structural adhesives are naturally brittle up to failure and elastic, in cases where their composites are combined with steel structures they are likely to collapse together with steel and form the popularly known composite action (Wang et al.,2017).

The advantages of applying fiber-reinforced polymer as showed in this paper includes stiffness, increased load carrying capacity, ductility, fatigue life and energy absorption. Studies and several research works have been concentrated on strength improvement effects of the fibre- reinforced polymer reinforced hollow steel tubular posts subjected stationary axial loading. Both the theoretical and experimental studies and research have been carried out so that to examine the functions of square hollow-section (Chellapandian et al., 2019).

Finite element modeling of FRP- steel joints

In 1950, was developed the Finite Element Method (FEM) for Study behavior and complex issues in engineering applications. This concept base on divides all element individually after that study this part only. FEM which helps to understand many of problem in especially for aeronautical engineering. This paper focuses on using CFRP which have many failures on the same part. It is possible for us to applied FEM on CFRM on joints.

The universally useful finite element or (FE) program ABAQUS was utilized for the investigation. A steel barrel with the stature h of 5000 mm, sweep R of 5000 mm, as well as the thickness ts of 5 mm was demonstrated as the reference case. The span to-thickness proportion R/t was 1000, delivering a medium-length chamber as per EN 1993-1-6. The estimations of Young's modulus, Es, and Poisson's proportion, ns, of the steel were taken as 200 GPa and 0.3, separately. The steel was accepted to have an elastic–consummately plastic pressure stanzas strain association with a yield worry of fy = 250 N/mm2. A uniform inward weight p and a vertical burden for every unit perimeter Nz were connected to the barrel. The base of the barrel was controlled in the spiral and pivotal bearings. The top edge of the barrel was controlled against pivot (Batikha et al., 2018).

Under axisymmetric stacking, these limit conditions guarantee that clasping happens at the base and model a chamber that is any longer than the degree of the neighborhood disfigurements associated with elephant's foot clasping (The barrel was displayed utilizing the two-hub axisymmetric universally useful shell component SAX1 which incorporates transverse shear distortion. Every hub has 3 degrees of opportunity). An axisymmetric component was legitimized as just axisymmetric breakdown was seen in past examinations that included checks for nonsymmetrical bifurcation (Feng et al., 2017). Non-straight elasto- plastic FE investigation was performed. The circular segment length strategy was utilized to follow the non-direct reaction in the wake of clasping. A work combination contemplates directed, from which a component size of 0:02 such a component estimate is far littler than that utilized where cubic components of scale 0:25 (El-Sayed et al., 2019).

Buckling strength of thin cylindrical shells without strengthening

For an undeviating metal tube-shaped shell with no reinforcing to oppose elephant's foot clasping, an upper bound to the quality might be taken as the condition where the von Mises viable pressure is come to outwardly surface of the shell (Selvaraj et al., 2017).The uniform metal cylindrical shell requires an upper bound and strength as the parametric conditions for the system to resist the existing elephant’s foot buckling. The condition also ensures that the von Miss stress is attained at the overall shell outside surface. The equation regarding the attainment of the aspect mainly indicated as shown below (Hu et al., 2017).

$$\sigma_{vM} = \sqrt{(\sigma_{mz} + \sigma_{bz})^2 - (\sigma_{mz} + \sigma_{bz}) \times (\sigma_{m\theta} + \nu\sigma_{bz}) + (\sigma_{m\theta} + \nu\sigma_{bz})^2} \quad \textit{(Equation 1)}$$

From the equation above theσ_{NZ}, is defined as the meridional membrane stress and $\sigma_{\mathrm{N}\emptyset}$ referred as the circumferential membrane stress. On the other hand, the $\sigma_{b\mathrm{Z}}$ mainly described as the meridional bending stress. Preferably, it is important to note that the latter stresses could be dormant in the equation above and this is depicted often when high internal pressure. Further to this, is von Mises Stress, mainly applied in this equation as the reference value (Batuwitage et al. 2017).

This the common term used in describing the failures associated with the local elastic–plastic and buckling. The failures often occur at the makeable base of the structural shells

of the cylinders. This is because the points are often subjected the sophisticated internal pressures as well as the axial force. The bucking failures is reported largely in the tanks which have been damaged as a results of the axial force coming from the earthquakes and thus, inducing the overturning moments. Furthermore, there is the likelihood that cyclic loading can also results to the elephant's foot buckle and thus, could lead to the completion of the circumference at the parametric tank bottom wall. Subsequently, there are scenarios under which the elephant's foot buckling often predicts the non-empty and thin silos when they elements are subjected the wind loads. Also, there is the formation of the local buckle at the adjacent boundary when the local bending effects tend to amplifies by the parametric co-existence resulting from the axial compression. Seemingly, there is the likelihood that smaller internal pressure often than not helps in increasing the buckling strength when they subjected to the axial compression (Chahkand et al. 2013).

Circular hollow steel section with CFRP design for design of local buckling would be used in measuring the influence of strengthening of CFRP

Experimental as well as design evaluation was investigated by (Haedir et al. 2011) of CFRP sheets that are externally bonded for circular steel tubular short columns strengthening as suggested methods of designs that may be used for cylindrical CFRP-reinforced steel tubular columns when subjected to compression.

Calculations of the capacities of axial section of CFRP-reinforced steel tubular short columns were deployed modular ratio concept. An assumption was made that the thickness of the layer of fiber was uniform and that there was enough bond between steel and the CFRP. The effective area of steel and supplanted cross sections given in present procedure for design of local buckling would be used in measuring the influence of strengthening of CFRP (Teng et al., 2007). The findings of the experiment suggest that using a combination of both longitudinal CFRP and hoop in a slender tube has the potential of enhancing attainment of capacity of yield of bare tube.

A comparison was made between the AS/NZS 4600, Eurocode 3 and AS 4100 and the ultimate capacities of the experiment in which a reasonable agreement was extracted. The evaluation has featured design curve increase with an increase in reinforcement factor,$\propto$. Besides, the changes in proportionating factor offer a quantitative comparison of effect of strengthening of reinforced columns (Lesani et al., 2013). The static load of such variables on CFRP-reinforced steel tubular columns capacity should be taken into

consideration to ascertain the design of the members is done effectively. The suggested rules of design below are usable for capacity CFRP-reinforced circular hollow steel section when subjected to axial compression.

Nu=Ns

$N_u = A_{ec}$

σ^c

Where Nu is ultimate axial compression

σ^c is the steel yield strength

A_{ec} is surface area of equivalent steel section

Bond behavior between CFRP and steel

1- Bond behaviour under dynamic load.

An elaborate comprehension of the mechanism of bonding is fundamental inn allowing the use of composites of CFRP for the purposes of strengthening of steel structures. The bond strength is often used in the determination of the performance of the bond. Bond strength is described as the ration of the maximum allowable load and the area of interface. Nevertheless, the relationship between a local bond and slip do not depend on the conditions of geometry and hence a model of a local bond-slip would be ideal for use in the measurement of the bond performance (Shaat et al., 2006).

In as a much extent research has been conducted on the relationships of bond slip of CFRP plat or sheet that are bonded to the joints of concrete, there has been limited research conducted on CFRP plate or sheet bonding to joints of steel. (Yu et al., 2012), (Chao et al.,2012), (Dai et al.,2005), (Nozaka et al.,2005), (Lu et al.,2007) and (Ishakawa et al.,2006) conducted both experimental as well as analytical investigation on the strength of the bond and offered a suggestion on the effective bond length that can be used in attaining perfect bonding for different dynamic and static loading conditions (Shaat et al., 2006).

2-Bond behavior under static load

The recent research conducted by (Fawzia et al.,2005) on investigations of the CFRP bonded steel plate duo strap joints as well as various numbers of layers of CFRP with various bond lengths underwent review. The carrying capacity of load of a given bond may be expressed using the equation below in which it is assumed the load is such that it is

linearly propositional to the length of the bond.

$P_{ult} = 0.8\tau w l_{eff}$

Where τdefines shear stress and w width of area of bonding

Nevertheless, experimental computation is needed to establish the shear stress, τ in the equation above. The predictions of this equation were further compared by Fernando et al. (2007) using the equation

$P_u = b_a \sqrt{2E_a t_a G_f}$

Where b_a defines the width of plate, E_a the elastic modulus of plate and t_a defining thickness of plate even as G_f represents the fracture energy of the interface.

From the equation, it is possible to offer a reliable prediction of the bond strength as long as the interfacial energy used adopted in the calculation is accurate.

CFRP strengthening of the channel columns by apply load carrying capacity of the ultimate load

CFRP-strengthened lipped cannel of column made of steel non-linear behavior as well as the load carrying capacity was investigated by Silvestre (2007). The aim of the investigation was to evaluate how the load carrying capacity as well as non-linear behavior of cold formed steel lipped columns of channel is improved by CFRP strengthening as well provided suggestion on the techniques that may be used in the calculation of the capacity of the ultimate load (Lesani et al., 2013). Nevertheless, the findings may change suppose there are changes in the surface preparation as well as adhesive material. Hence, unique procedure for design need to be developed to standardize equations of design.

Square hollow section design with CFRP under a load local buckling

The axial capacity as well as the design of a steel square hollow section with a thin wall and strengthened using CFRP that has been externally bonded was investigated by (Bambach et al., 2009). Spot-welding was used in fabrication of the square hollow section and the ration of width to thickness of the plate was in the range of between 1.1 and 3.2. Investigations were conducted into two various layouts of matrix of CFRP and the findings illustrated that local buckling was delayed by applying CFRP to the thinner sections and thereby leading to substantial increase in the axial capacity, elastic local buckling and strength to weight ratio of the members of the compression.

A method of design is then established in which the steel- CFRP sections theoretical elastic buckling stress is adopted in the determination of axial capacity and is illustrated to be comparing well with results of the test (Kalavagunta et al., 2014). A reliability analysis conducted on method demonstrates it is suitable for use in design. The suggested rules of design are shown:

f_{cr} defines elastic buckling stress on the curve of load –axial displacement, E is the Young's modulus, f_y defines the yield stress, b is width of the plate, t thickness of the plate and υ is Poisson's ratio.

(Equation 2)

$$\lambda = \sqrt{\frac{f_y}{f_{cr}}}$$

$$f_{cr} = \frac{k\pi^2 E}{12(1-\upsilon)^2}\left(\frac{t}{b}\right)^2$$

Prediction of capacity using the theory of composite plate

(Equation 3)

$$t_t = t_s + t_{CFRP}$$

$$E_{CFRP} = \frac{E_a t_a + E_{cf} t_{cf}}{t_a + t_{cf}}$$

$$P_{uc} = \rho_c A_s f_{ys}.$$

Ability the CRFP to stabilize members and resistance lateral displacement forces

There was the magnificent factor which supports CHS to immovability under lateral impact load around 29 % if analogy on a sample which has not covered CFRP his parts(Alam *et al.*, 2017)**.** Moreover, the position of CFRP which can effect on capacity lateral load which can be respected, from mulita of experiment proof that the longitudinal axis was more efficacious than another.

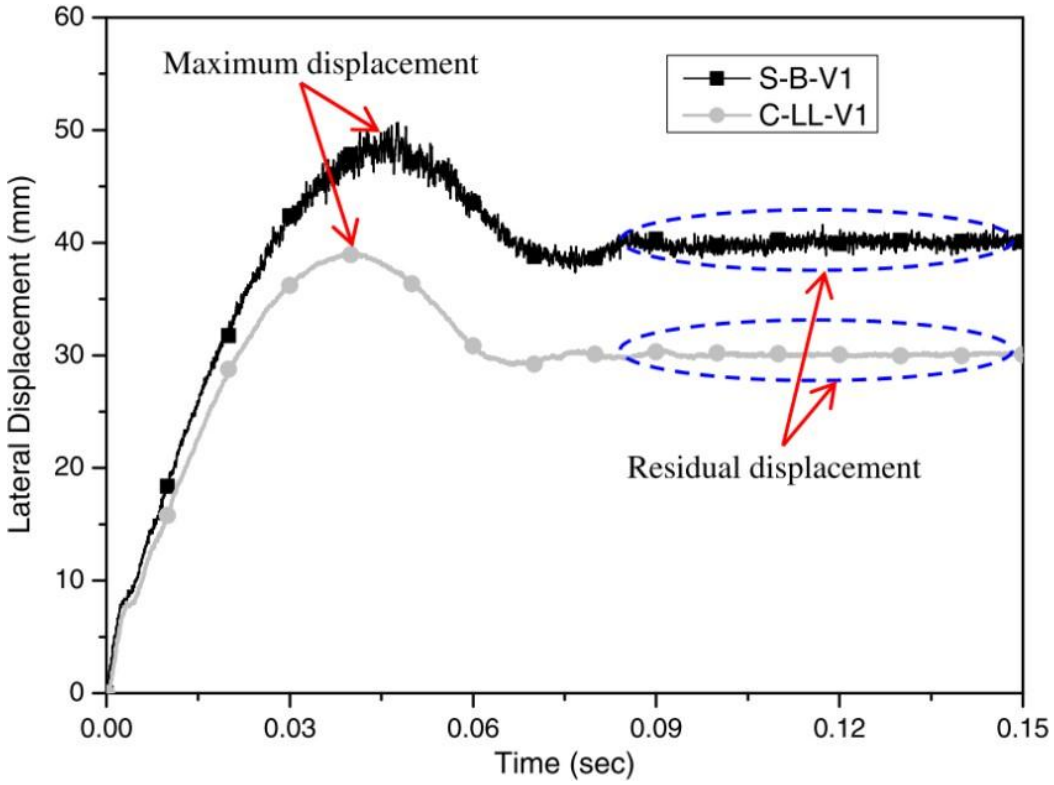

Figure 1: Lateral-displacement time histories of bare and CFRP-strength- end specimens (Alam *e*t al., 2017).

Direction. Never less, it is can to reduce many of the cracks results of lateral forces. it is possible for us to represent Kinetic energy force by:

$$E_k = \frac{1}{2}MV^2$$ ***(Equation 4)***

Where:

M = total mass of impactor; V = initial impact velocity

The fig below which show us the relationship between variance Drop-Hammer Impact Test Results with lateral displacement result of changing heights for multi specimens:

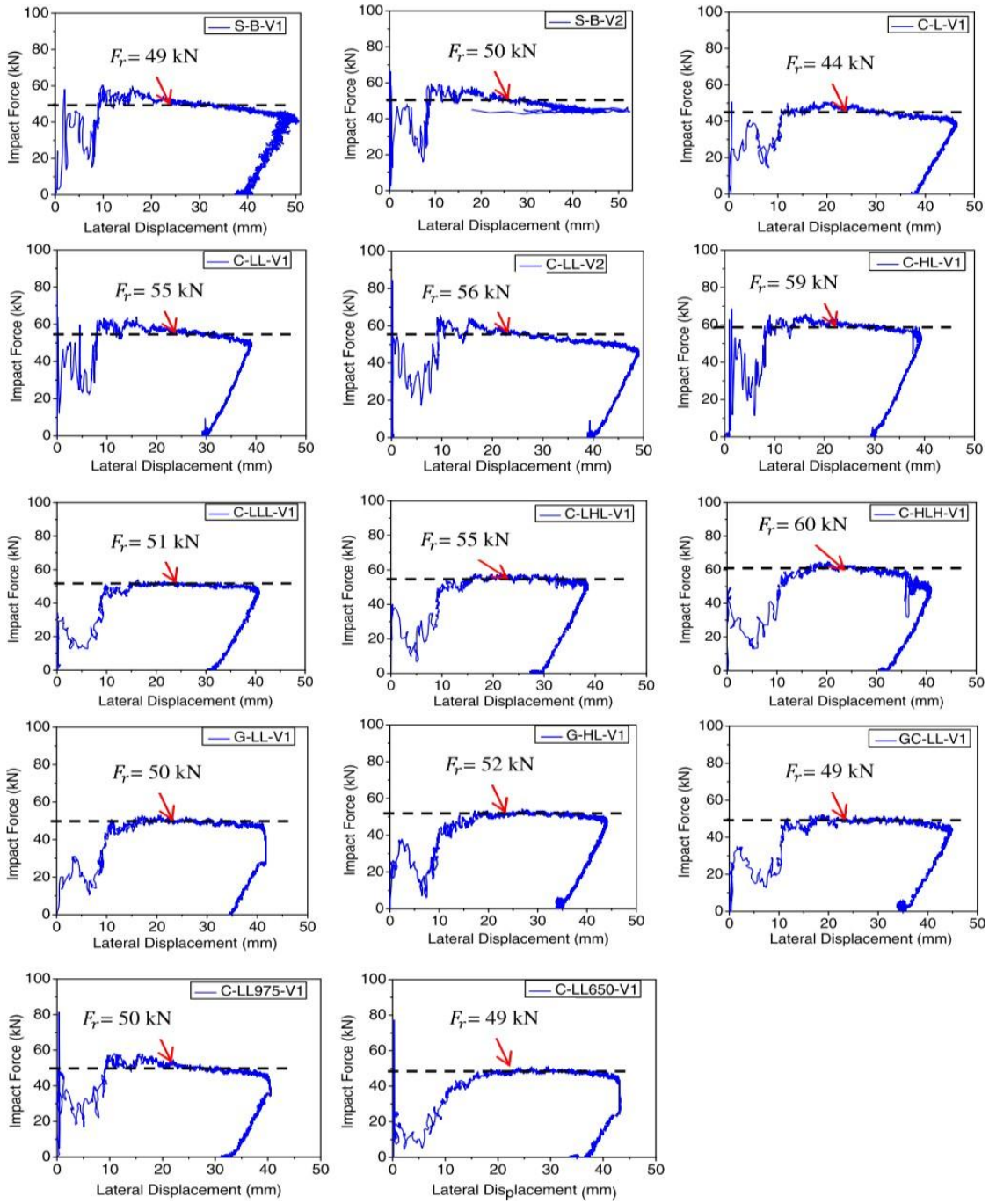

Figure 2: Impact-force versus lateral-displacement responses of all test specimens (Alam *e*t al., 2017).

FRP parameters for achieving the highest loading capacity

The FRP sheets should serve as the circumferential restrain in line with the area. In this analysis, the von Mises stress are considered to be at the peak and thus, taken as maximum. The consideration of the von Mises maximum likely to trigger the local elastic-plastic process and thereby leading to collapse as indicated in the figure below (Gao et al., 2013).

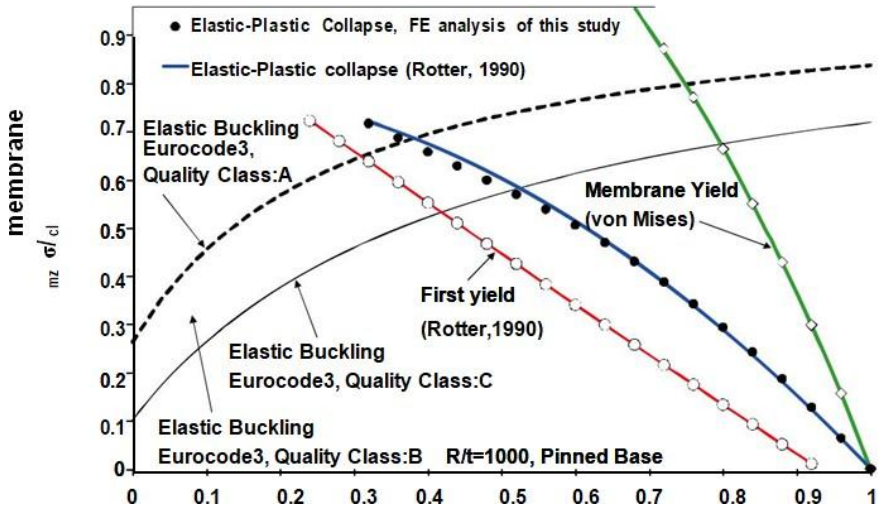

Figure 3: Showing the Normalized internal pressure pR/tfy (Lesani et al., 2014).

Moreover, it is important to note that the circumferential restraints main objective is to help in increasing the overall axial capacity. The analysis has to be taken at the elastic– plastic collapse point (Chen et al., 2016). Further to this, there could be the extension on the aspect and thus, it could extend to the elastic buckling shell strength end. Moreover, the possibility of increasing the makeable elastic buckling shell strength mainly conducted via the introduction of the wrapping whole shell of the FRP. The process is neither economical nor have any great static load as thus, it always avoided in many occasions.

(Park et al., 2013) reported that the elephant's foot buckling and capacity via the application of the local FRP is an important analysis. It will help in offering the necessary strengths near the bottom boundary but within the parametric small zones. It is therefore important to note that there different achievable maximum and strengthening which the FRP can assist in attaining. Some of them include enhancing the elementary axial load capacity and this can be done to either the yield strength of the membrane or to the elastic buckling strength. The overall goal of the process is always attained. This because the objective of the process is to help in preventing the occurrences of the elephant's foot buckle from happening before the other makeable failures modes have been recorded (Kabir et al., 2014).

There are three and vital parameters which are used to determine the effectiveness associated with the method employed in the process. The parameters comprises of the following t_f, h_f as well as x_f. The experiment uses the two parameters as fixed variables while the other one is then varied until the overall optimum values required are obtained.

The parameters are used interchangeable in line with the fixed and variable ones. For instance, the figure below indicates the analysis of the buckling strength for the makeable three different elevation ratios in line with the reference FRP and the cylindrical shell. The analysis incorporated the application of the k = 0.46 and $x_f/ l = 0$. It is evidential that the height ratio of the FRP is demarcated to be $h_f/ l = 0.75$ (Feng et al., 2014).

This indicates that the FRP have achieved the required maximum enhancements as far as the buckling strength is concerned. Subsequently, most literatures have reported that axi-symmetric FE models only helps in predicting the collapse failures associated with the axisymmetric elastic–plastic. The norm is applicable in the perfect cylinders. However, it does not apply in the non-axisymmetric elastic split failure. The analysis answers the questions as to why the predicted collapse strengths of the elastic–plastic are often higher as compared to the plotted elastic buckling strength (Parket al., 2013).

Corrosion effect on CFRP-CHS steel member

The length of correction for the tube was Lc / Dn = 1.0 to 3.0. Where Lc = length of corrosion and Dn is the nominal diameter. In addition, the ratio examined thickness-to-The external diameter is D0 / ts = 20.3 to 93.6. There were many of benefits of using CFRP to support CHS which have of steels corrosion. Moreover, it is able to increase CHS around 282% which have severe corrosion about 80% and load carrying capacity is 97%(Mohamed Echeloning, 2015). Moreover, The mechanical properties for material which consider the main reason to get high performance. Adding CFRP on both direction able rising up strength to resistance from 40% to 80%(Mohamed Elchalakani., 2016).

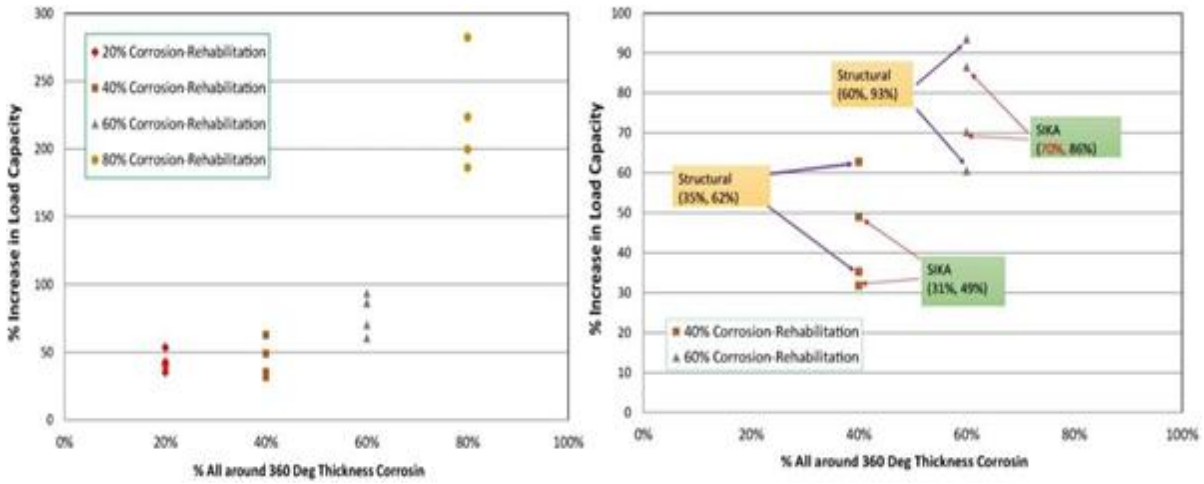

Figure 4: Increasing strength of CFRP for rehabilitation series for Sika and Structural (Mohamed Elchalakani, 2016).

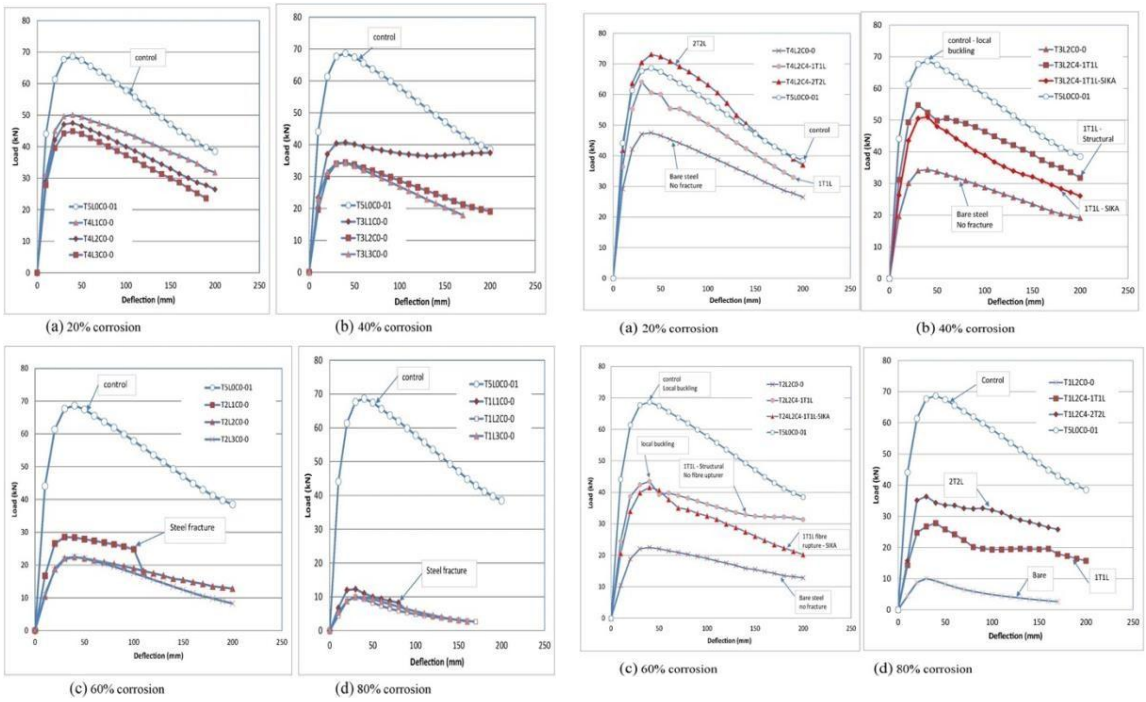

Figure 5: Response of the load-deflection on Lc on for bare specimens with different corrosion percentage (Mohamed Elchalakani, 2016).

CFRP-strengthened steel circular hollow sections

The planning approach for empty steel segments was utilized to build up the structure bends for CFRP-reinforced steel CHS made with shifting steel yield pressure. The impact of the measure of CFRP, modulus of the flexibility of the band CFRP and steel yield weight on the quality of fortified steel CHS has been featured. The examination has demonstrated that the conditions are expanded for cylinders fortified with a higher measure of CFRP. The Eurocode 3 quality bends are lower than those of AS/NZS 4600 and AS 4100 in the thin range. The examination has portrayed the expansion in the quality bend with the increment of the fortification factor α. Further, the proportioning factor (Ç) for the band carbon strands gives a quantitative correlation of the dimension of solidarity improvement of the fortified segments. The impact of these factors on quality should be considered to guarantee the successful plan of CFRP-fortified steel round empty areas. The analysis mainly summarized as indicated in the table below:

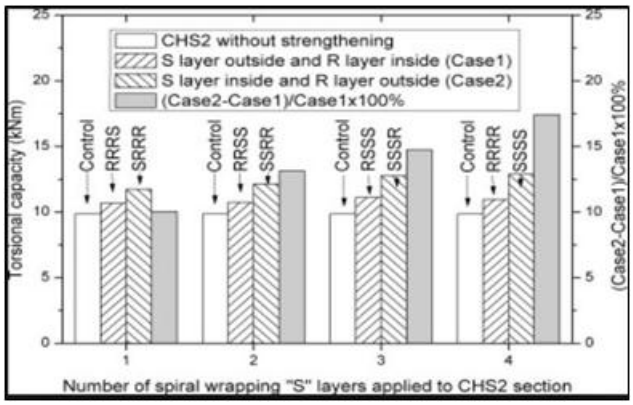

Figure 6: Graphical analysis of the CFRP-Strengthened Steel Circular Hollow Sections (Keykha 2017).

Tubular structures and joints

Most of the tubular structures are made of the makeable thin-walled hollow and structural sections and this as a result of the attractive appearance and the excellent mechanical properties which they have in the long run. The application the tubular and thin-walled steels widely utilized in the civil engineering works because of the mechanical properties. The structures often have different structural shapes in line with the tubular joints. Some of the commonly used joint types include T-joints, N-joints as well as K-joints. The joints mainly designated and defined as the connection regions which exist at different hollow sections. The joints also regarded as the crucial and critical tubular structural sections (Alam et al., 2017). The analysis regarding the evaluation mainly indicated as shown below

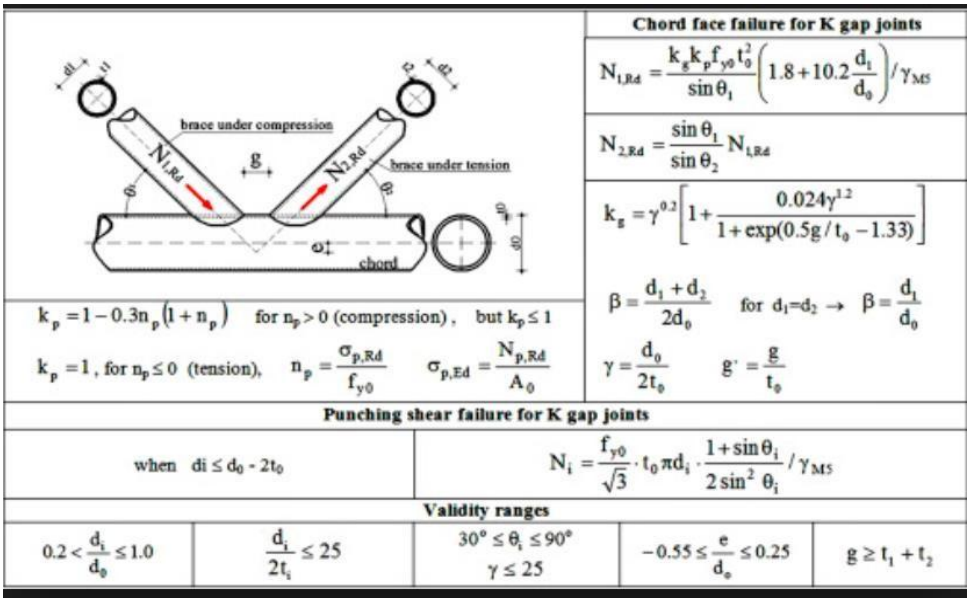

Figure 7: Figure showing the Tubular Structures and Joints (Alam et al., 2017).

The past analysis has reported that large volumes of tubular elements have been applied and used in the civil engineering works. Further to this, there is the need to carry out repairs as well as strengthened the tubular structures as result of the declining performances of the norm. Also, increased loading on the elements, raises another genuine concerns as to why it is important to carry repairs and strengthened the structures in the long run. Traditionally, most people prefer the act of utilizing the bolting, grout cement and welding as the metallic stiffeners in the tubular joints process. The process help in lowering the internal voids associated with the joints in the long run. Conversely, the elements have no immense advantages in the in- service structures in the recent application. Thus, the application of the Fibre Reinforced Polymer or (FRP) offers more attractive and viable means of strengthening the tubular structures. The application of the Fiber Reinforced Polymer is gaining momentums grounded on its mechanical properties. For instance, the Fiber Reinforced Polymer has both the installation ease as well great durability as well as has vast range of relevant development techniques. The analysis in line with the factor reduction mainly illustrated as indicated in the figure below.

7. Reinforcements	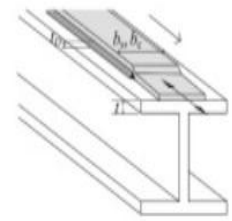	End of long doubling plate on beam, reinforced welded ends ground (based on stress range in flange at weld toe): $t_D \leq 0.8\,t$ $0.8\,t < t_D \leq 1.5\,t$ $t_D > 1.5\,t$	 71 63 56	Grade 2
	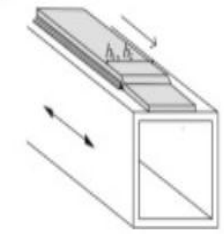	End of reinforcement plate on rectangular hollow section; wall thickness t < 25 mm	50	Grade 2
8. Flanges, branches and nozzles	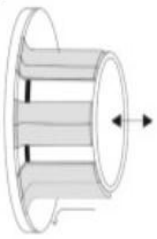	Stiff block flange, full penetration weld	71	Grade 2
		Stiff block flange, partial penetration or fillet weld: toe crack in plate root crack in weld throat	 63 36	
9. Tubular joints	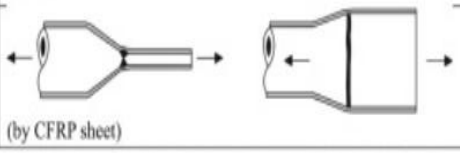 (by CFRP sheet)	Tube-plate joint, tubes flattened, butt weld (X-groove): Tube diameter < 200 mm and plate thickness < 20 mm	63	Grade 2

Table 1: Showing the Factor Reduction and Reinforcements (Keykha et al., 2019).

Rather than applying the Fibre Reinforced Polymer in the reinforcement and in the process of profiling, it also has vast utilization in the repairs of the existing structures. This application primarily defined as the retrofitting applications. The norm is largely applied in the concrete, masonry as well as in timber structures. Presently, there is increased application of the Fiber Reinforced Polymer in the metallic structures. In essence, the applications of the Fiber Reinforced Polymer in the strengthening of the metallic structures have continued to gain immense momentums. The application mainly witnessed in the metallic beams, walls, columns, as well as in the pipeline works. The excellent characteristics in line with the corrosion resistance and the shape flexibility have increased its application in the rehabilitation of the overall tubular structures. The application is grounded on the high FRP efficacy and the externally bonding of the parametric FRP (Lesani et al., 2013).

However, there is no concrete research which establishes the application of the Fibre-Reinforced Polymer in line with the utilization of the joints. Furthermore, it is evidential that the tubular structures often have complex geometry in the in-services structures. Thus, the application of the Fibre Reinforced Polymer is important and beneficial in most cases as compared to the tradition methods in the long run.

Tabular K-joints of GFRP composites are largely applied when repairing the fatigued-cracked CHS of the truss of joint aluminum. The analysis of both the fatigue and the static tensile mainly performed to show and demarcate the GFRP effects in line with the ultimate damages as well as the fatigue life of the material. Preferably, there was the proposal to apply the FRP in the installation of the materials to repair the makeable damages in the CHS aluminum as a result of the fatigue. The experimental results indicated that there was full strength recorded in the joints and the restoration in the K-joints mainly recorded due the application of the CFRP. The application of the GERP indicated that the restoration levels could rise up to 70% of the overall strength restored. However, there was investigation on the static load and the damages which the FRP has on the tubular K-Joints; there are fewer installations which the researchers have embarked on appraising the FRP effects on the viable undamaged tubular K-Joints. It requires maximum rehabilitation and this is due to the under-strength structural members, deteriorations, and the load demands increase. It is important report that, the undamaged failure modes aligned to the K-joints have specified FRP and uncertain installation

techniques as opposed to the damaged joints. Thus, it is important to have the designs carried out in line with the overall failure modes to hasten the strength in the joints and thereby increasing efficiency. Largely, there are various failures which are likely to be recorded for different tubular joints on a daily basis. Some of the failures include weld failures, local braces failure, chord punching shear as well as chord plasticization. Preferably, the design and the application of the various specifications in line with the engineering standards ensure that major failures are often eradicated in systems. The design principles therefore, play a major role in avoiding these failures and thus, ensure that only two major failures are left behind. The two key failure modes considered in the process include the chord punching and plasticization shear. Notably, the two mode failures possess different traits. Therefore, it is evidential that FRP installation and the technique proposed in the process may not be sufficient enough to help in averting the undamaged strengths in the tubular K-joints. Thus, in the recent days, there have been proposal have the techniques which can be used in handling the FRP installation as well as undamaged tubular K-joints. In essence, this paper embarks on the practical application of the CFRP installations and techniques to assist in strengthening the undamaged CHS tubular K-joints. The techniques incorporate the application of both finite elements (FE) as well as experimental methods in designing and investigating the overall CFRP effects. The appraisal encompasses on the ovalization, ductility, displacements and failure modes. In the experiment regarding the norm, three key tubular gaps and K-joints have to be wrapped with the makeable CFRP sheets. The wrapping must be conducted differently as well as the tests have to be conducted via the application of static forces in the critical braces. Notably, the process uses whilst joints as the key notch for reference specimen and these are important for the comparison purposes. The three-dimensional (3D) FE models mainly utilized for the purposes of conducting the numerical analysis.

The verification process of the FE model is not only important but also critical. The verification process incorporates the comparison between the FE predictions and the experimental results gathered. The figure below indicates the results compared in the process of the verification.

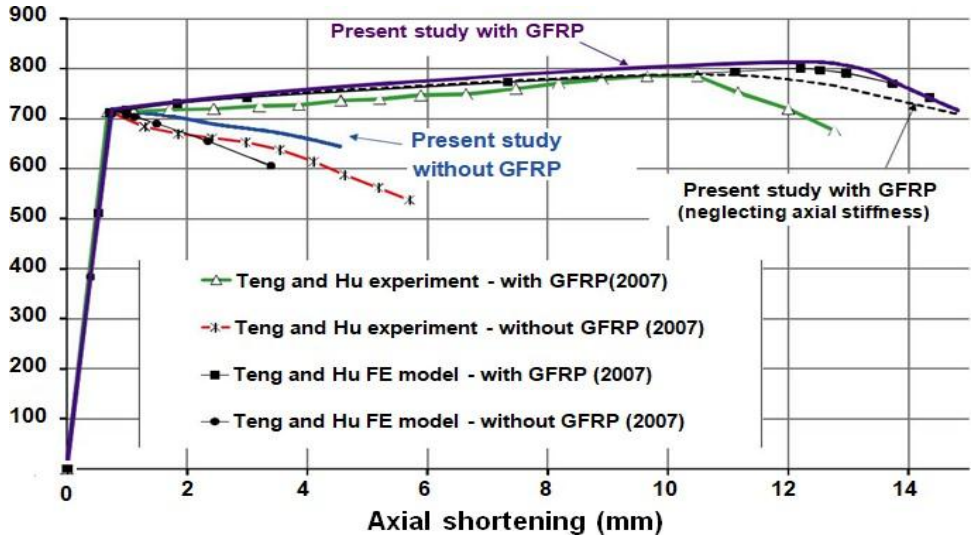

Figure 8: Figure showing the Load–axial shortening curves of a thick cylindrical tube (Zhao et al., 2013).

The experiment primarily conducted with the objective of determining the FRP confinement and effectiveness associated with the steel tubes. The practical task incorporated the utilization of the glass fibre reinforced plastic also denoted as the (GFRP).

Preferably, the experimental modeling included the utilization of the fixed-based steel tube which had a height of h =450mm, thickness of ts = 4.2 mm as well as radius of R =80.4mm. Also, the values for the Young's modulus, the yield stress as well as the Poisson's ratios mainly established as 201Gpa, 335Mpa as well as 0.3 respectively. On the other hand, the train hardening elastic modulus value mainly established to be 5%. There is the consideration that the tube used in the process is thick and it has R/t ratio of approximately 19 (Dong et al., 2013). Moreover, there is the modeling of the 0.53 mm thick (tf) three-ply GFRP jacket on the surface of the tube height as indicated in the experiment. On the other hand, there is the modeling of the GFRP sheet as this carried out as orthotropic material with the Efu=80.1 GPa, nfuz=0.35, Efz=3 GPa, and nfzu=0.013. It is important to note that both the Teng and Hu conducted their experimental analysis via the application of the B33 elements and this was done in the ABAQUS oriented appraisal. They used the hop direction to assist them in modeling the S4R shell and FRP elements. In addition, the B33 is defined as the bi-cubic beam and elements which has 6 DOFs as per the node. The examination of the B33 utilizes its element height as that of the shell element. On the other hand, the S4R is defined as the four-node doubly arched with the

general-purpose shell. It helps in reducing the hourglass of the integration control as well as the transverse effects of the shear deformation. The nodes applied in the system are situated in the manner that each comprises of the three rotations and three displacements. The figure above indicates the load-deflection curve for the makeable pair of the practical task. The experiment is designed in a manner that it does not have the GFRP strengthening (Yang et at., 2013).

There were two key testing load capacity applied in this experiment. The value for the latter was estimated be 717.5kN whereas the value for the former mainly depicted at 782.2kN. The FE curves for both the HU and the Teng were also illustrated. There was also the incorporation of the of the FE model curves predicted from the study. Both the Teng and the HU models for the GFRP via the application of the beam elements indicated that the predictions for the loadings capacities were 800 kN as well as 709 kN respectively. The evaluation was conducted for both the specimens having the FRP strengthening and the one which lacked the norm. On the other hand, there was the modeling of the GFRP using the amicable shell elements and this predicted the corresponding values of the loading capacities as 787 as well as 709 kN respectively. The values were recorded in the analysis which neglected the FRP vertical stiffness (Efz = 0). Thus, the experiment indicated the predicted values were very close to the real time values tested. Thus, also the values indicted positive GFRP strengthening.

Experimental of CHS tubular beams CFRP-reinforced steel

The external holding of carbon fiber strengthened polymer (CFRP) sheets to the fringe of steel roundabout empty areas (CHS) is a generally new method for fundamentally improving such segments. Plan of CFRP sheets for reinforcing cylindrical steel segments requires the forecast of the limit of kept steel round segments (Alam et al., 2017). The literature exhibits a planning technique for assessing the limit of CFRP-reinforced steel CHS exposed to twisting. The band FRP decreases the impact of neighborhood clasping by limiting the cylinder divider. The effect of loop CFRP considered in the proposed strategy by accepting its modulus of versatility as an extent of the elastic modulus of longitudinal CFRP. The excitation of the longitudinal CFRP limits the impact of nearby locking in the cylinder divider, which at last expands the neighborhood flexural firmness and quality of the cylinder (Alam et al., 2017). The incorporation of the static load of fortifying parameters in current plan rules, quite the Australian Standards AS/NZS 4600 (2005) and

AS 4100 (1998) and the European Standard EC 3, is examined. The reinforcing static load considered here are those that emerge from fluctuating measure of CFRP, modulus of the flexibility of the loop fiber and steel yield quality. Quality bends for composite CFRP-steel CHS are given to delineate the degree of improvement with the sort of the parameter (Keykha, 2017).

The FRP-Strengthened cylindrical shells modeling

The application of the cylinder indicates that the FRP sheet with the overall height denoted as hf can be bounded to the cylindrical external surface shell. The bounding can be started at the level which has to be at height higher tha the base and it is demarcated as xf. It is important to treat the FRP sheet as the orthotropic as per the young's modulus Efu when applied as the circumferential direction. Further to this, both the Efz as well as nfuz are considered as the meridional and poisson's ratios directions respectively. The modeling of the FRP lamina mainly conducted via the utilization of the SAX1 element and this is noted as the axisymmetric shell of the two-node element. In the modeling, the assumption is taken that there is the perfect bond existing between the FRP sheet and the cylinder (Hu et al., 2013).

Specimen fabrication and material properties

The figure below indicates the specimens' geometric configuration and this is fabricated with the critical two seamless steel type tubes. The common used steel type utilized in this process is the low carbon which is grade Q235B. The low carbon steel mainly estimated to have a minimal yielded stress which is specified to be 235 MPa as per the GB/T700-2006 analysis. The process involves the full adoption of the penetration welds and this must be carried out as per the manufacturing specimens. The process mainly carried out using the gas metal arc welding technique. The technique applied in the process encourages the application of the prequalified welding procedure drawn from the United States of America. It also incorporates the utilization of the decisive *Welding Society (AWS) code (AWS 2008)*. The fabrication of the steel specimens mainly conducted by the manufacturer and the individual also examines all the associated errors as well as designed the mechanism of curbing the same in due course. The analysis of the fabrication process mainly illustrated using the figure below.

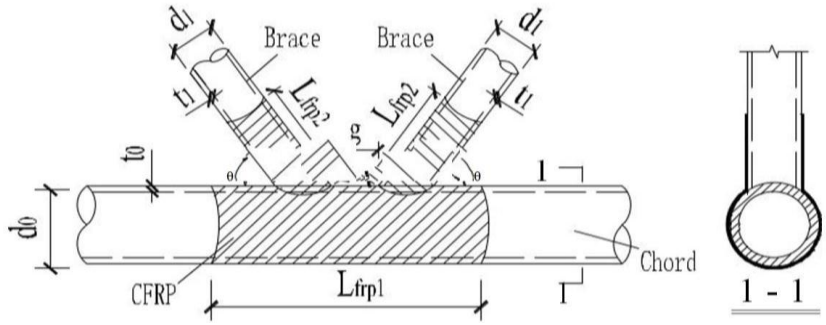

Figure 9: Indicating the Dimensions as well as parameter descriptions of a braced gap K-joints (Keykha 2019).

Also, the test results specimen analysis can be summarized in the table as indicated below.

Test specimens.									
Joint	**Remark**	**Dimensions of steel tubes**				**Parameters of CFRP sheets**			
		CHS chord d_0 t_0 (mm)	**CHS brace d_1 t_1 (mm)**	**Degree 0 (degree)**	**Gap g (mm)**	**Unidirectional CFRP**		**Bidirectional CFRP**	
						Layer	**Length L_{frp1} (mm)**	**Layer**	**Length L_{frp1} (mm)**
J0	Reference joint	219 8	133 6	55	40	0	0	0	0
J1	Strengthened joint	219 8	133 6	55	40	3	300	4	600
J2	Strengthened joint	219 8	133 6	55	40	3	300	2	1000
J3	Strengthened joint	219 8	133 6	55	40	3	300	4	1000

Furthermore, the geometric configuration often applied in the examination of the steel tubular mainly illustrated as indicated in the figure below

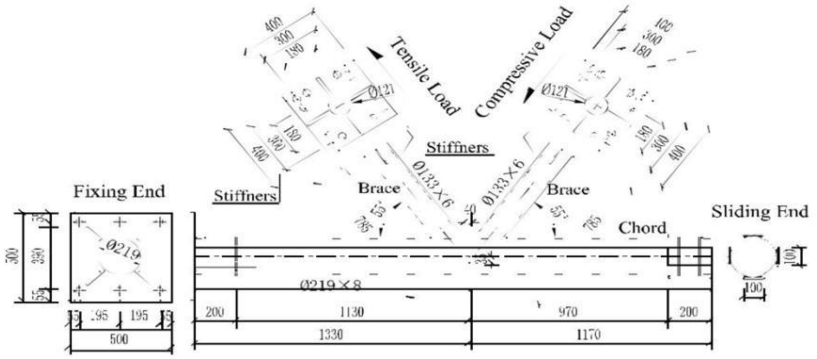

Figure 10: Figure Showing the Geometric Specimen Configuration (Katrizadeh et al., 2019).

Moreover, the steel tubes measured properties are also critical and important for the evaluation in line with this project. The various properties as per the values mainly summarized and tabulated as indicated below (Feng et al., 2019).

Member	Thickness t (mm)	Yield strength f_y (N/mm^2)	Tensile strength f_u (N/mm^2)	Strength yield ratio f_u/f_y	Elongation δ (%)	Yield strain μs	Density y (g/m^2)
Brace	8.07	298	480	1.61	29	1932	300
Chord	5.46	310	473	1.52	26	1552	380

The reinforcement of the metallic tubular joints can utilize both the GFRP and the CFRP. However, most analysis utilizes the CFRP and this because of the higher strength and elastic modulus which they have in meantime. Essentially, the fundamental objective of including the FRP reinforcement is to bridge the K-joints. Thus, the norm will help in lowering the delays associated with the primary failures and modes. The aspect is carried out by the means of ensuring that there are confinements for the steel substrate deformation (Abu-Sena et al. 2019). The analysis indicates that CFRP assists in providing the stronger enhancements as compared to the GFRP and this plays a fundamental role in gapping the K-joints. It also facilitates the attainment of the higher load bearing and capacity in the system. The experiment majorly applied two typical and CFRP sheets (Djerrad et al., 2019). This enables the specimens to be strengthened. The two typical CFRP sheets applied include bidirectional and the unidirectional. There is the knitting of the fibers in one direction for the unidirectional CFRP sheets whereas the carbon fibers mainly knitted into makeable two orthogonal directions as far as the bidirectional CFRP sheets were concerned (Ghaemdoust et al., 2016).

The selection of the CFRP sheets dimension were carried out decisively and this aimed at decreasing the fiber cutting work and thus, alleviating disturbance of the fiber materials. The unidirectional CFRP sheets mainly delivered in different rolls as 0.1, 0.2 and 0.3 widths respectively. On the other hand, the width used in the bidirectional sheets was 1m width. Moreover, there was the adoption of the structural adhesive and these comprises of the curing agents as well as the epoxy resin. The ratio utilized in the process mainly estimated at 1:3 respectively (Dlugosch et al., 2017).

Preferably, there is also doubling checking of the both the mechanical properties as well as the dimensions of various materials. Also, the average results values mainly taken as the

reference and this applies when carrying out both the numerical and experimental analysis. The analysis and the values for the mechanical and dimension properties mainly indicated as illustrated in the figure below (Shakir el at.,2016).

Table 2: Table Showing the Measured Properties of the CFRP Sheets (Islam et al.,2014).

Measured properties of the CFRP sheets.					
Member	**Thickness t(mm)**	**x-direction**		**y-direction**	
		Modulus E_x (GPa)	**Tensile strength S_x (N/mm^2)**	**Modulus E_y (GPa)**	**Tensile Strength S_y (N/mm^2)**
Unidirectional CFRP	0.167	297	2373	3	48
Bidirectional CFRP	0.211	134	1649	134	1649

The table above indicates the essential and vital steel tube mechanical properties as well as the CFRP sheets. The evaluation of the mechanical properties mainly carried out via the application of the uniaxial tensile series. The analysis incorporated the utilization of the braces as well as the chords coupons in keeping with the parametric GB/T228.1-2010. Correspondingly, the analysis was also appraised as per the GB/T 3354-2014 and in the analysis the mechanical properties mainly determined by the incorporation of the CFRP sheet coupons. This examination includes the use of the CFRP sheets hardened and combined with the elementary structural adhesive sheets for a defined duration. The tabulation of the above description and the results mainly indicated as shown in the table below (Parvin et al., 2014).

Table Showing the Resin and FRP Properties (Sundarraja et al., 2014).

Material type	**Material properties**		
	Properties		Value (unit)
CFRPa	Tensile modulus		230 (GPa)
	Tensile strength		3400 (MPa)
	Shear modulus		7.17 (GPa)
	Shear strength		68 (MPa)
	Poisson’s ratio		0.3
Resin	Tensile modulus		3443 (MPa)
	Tensile strength		48.4 (MPa)
	Tensile elongation		1.60%
	Compressive strength		87.9 (MPa)
	Flexural strength		88.1 (MPa)
CFRP/epoxy	*G T*	fracture toughness	91.6 (kJ/m^2)
	1*C*		79.9 (kJ/m^2)

	G C	fracture toughness	
	1*C*		0.22 (kJ/m^2)
	G T	fracture toughness	
	2*C*		1.1 (kJ/m^2)
	GC	fracture toughness	
	2*C*		

On the other hand, the above analysis mainly represented in the graphical diagram as shown below (Cascardi et al., 2016).

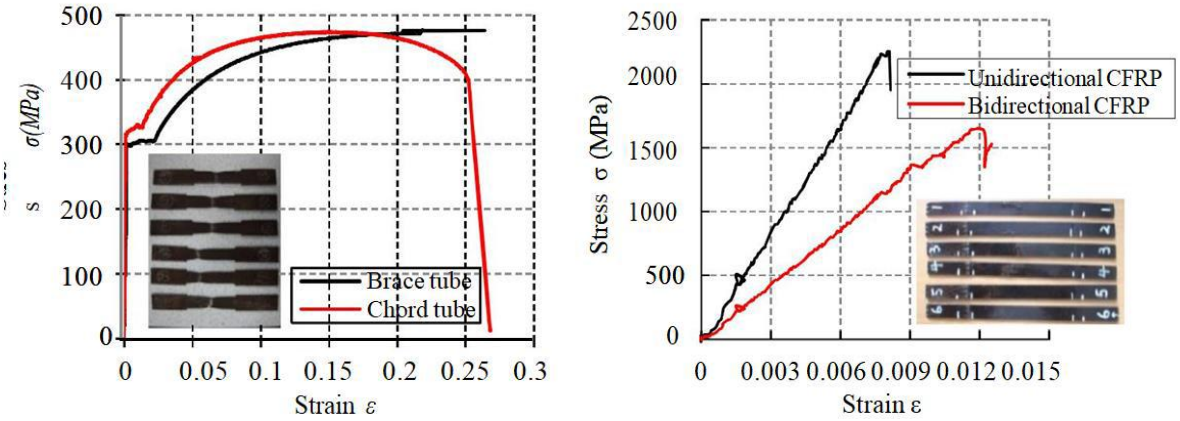

Figure 11: Graphical Diagrams Showing the Coupons as well as Typical Stress–Strain Curves (Kalavagunta et al., 2014)

V. Research Gap

There has been inadequate research on the steel circular hollow section evaluation result of many of analysis has recommended the application of the FRP materials with CHS. There is the continued need to appraise the restraining static load which the sections of the CHS form steel will have in line with the CFRP. Thus, the research forces on the strengthening of the CHS using the Bidirectional FRP and their overall benefits in the structural and civil engineering works.

I. CHAPTER THREE

II. EXPERIMENTAL PROGRAM AND RESULTS

1. Introduction

There has increased utilization and acceptability of the fibre-reinforced polymer in the CHS as far as the structural engineering tasks and the overall community is concerned. The key notch advantages which have fostered the application include the high strength-to-weight rations, high levels of corrosion resistance as well as minimum service interruption in the construction. Furthermore, the FRP retrofitting and strengthening of the steel structures

continues to have immense benefits based on their ability overcome the conventional problems as well as the innovative composite constructions which they add the metallic structures and processes. The research has also indicated that the FRP have the ability deform in correlation with steel and thereby creating the composite action. The norm is important since it applied in the repairs as well as in the strengthening of the steel structures. This helps increasing the stiffness, ductility, fatigue life, energy absorption as well load bearing capacity of the structure.

Resource: Samaro.fr. (2019). [online] Available at: https://samaro.fr/pdf/FT /Araldite_FT_420_AB_EN.pdf [Accessed 3 Jun. 2019].

Table 3: Material Properties of Steel, CFRP and Adhesive.

Property	Steel tube	CFRP	Adhesive
Elastic modulus (GPa)	211	230	3
Tensile strength (MPa)	366	4900	23
Yield stress (MPa)	317	--------	-------
Thickness of FRP (mm)	----------	0.166	-------

1. Papering specimens and diving to groups

Indeed, we have **Fourth Groups** specimens which as following:

Group# 1: There were five specimens which cutting for 420mm of length and clean via chemical liquid which is called “Diggers” (fig:11). It has the ability to remove any oil on the surface tube after that we can be sander surface for CHS which will past on CFRP by sander machine (facing tube area on the sand and high-pressure air as (fig:11).

Figure 12: Chemical liquid Diggers and sander machine.

Moreover, it is a possible for us to cleaner specimens by asternal water before wrapping.

Figure 13: Specimens after clean via sander pester.

On other hand, this **group# 1** which divided areas for CFRP as following:

1- One simples for 50mm. 2- One simples for 100mm. 3- One simples for 150mm. 4- One simples for 200mm. 5- One simples for 250mm.

Furthermore, we distribute rags the CFRP as dividing above and (fig:15) show us that:

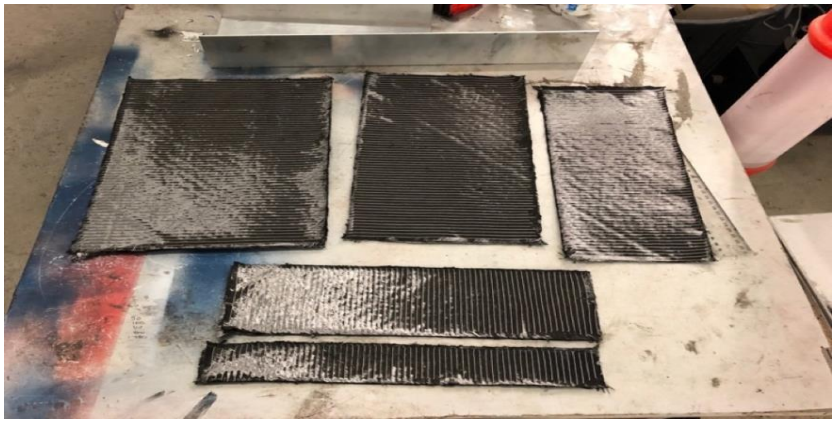

Figure 14: CFRP after cutting rag.

To paste rag CFRP with CHS, we need mixed adhesive which called: 1-Aradlaite **420 A** (yellow). 2-Araldite **420 B** (blue).

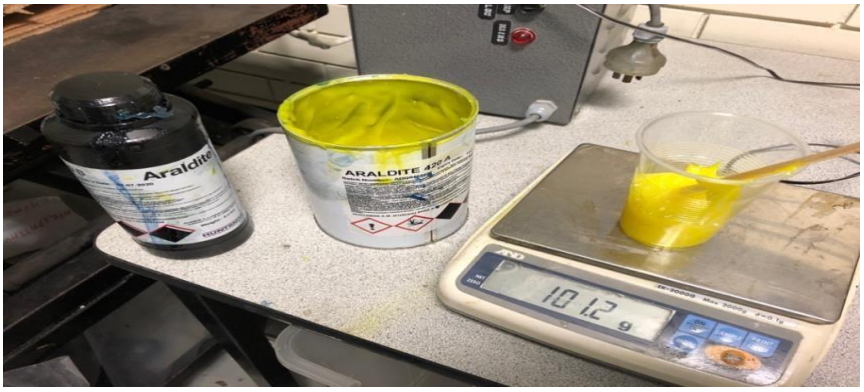

Figure 15: Adhesive bolts.

The final steps(Fig:14), which is sensitive because it need mover to practise to warp and how can stays samples in excellent environmental "curing" which needs about one week to achieved bond between adhesive and CFRP:

Figure 16: Specimens after wrapping and curing.

Group# 2: We have five specimens which cutting for 420mm of length and reducing thickness via "Lathing machine " (fig:15) for five size 20 mm, 70 mm, 120 mm and 170 mm per width while 0.6 mm reducing diameter of 4.2mm. The main cause to chosen 0.6 mm reducing od thinness, the many case study which confirmed that "the rust steel which factor of weather condition and time to regard this case studies which said that 15% (4.2mm *15% =0.6 mm) of steel lost result of corrosion or rust steel Accordingly, we can complete warping as method for Group#1 as fig: 19.

On other hand, this **group# 2** which are reducing areas 0.6 mm of thickens as following:

1- Two simples for 20 mm which warp with 50 mm of CFRP.
2- Two simples for 70 mm which warp with 100 mm of CFRP.
3- Two simples for 120 mm which warp with 150 mm of CFRP.
4- Two simples for 170 mm which warp with 200 mm of CFRP.

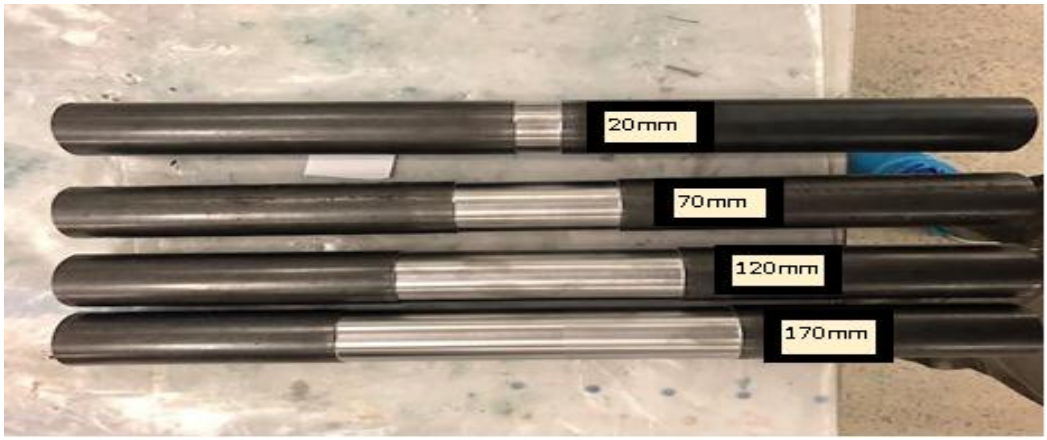

Figure 17: Lathing "reducing" thickness for 20mm, 70mm, 120mm, 170mm.

Likely, the second steps to cover adhesive by Aradlaite **420 A and B adhesive.**

Figure 18: Specimens which lathing before wrapping.

Group# 3: We have five specimens which cutting for 420mm of length and reducing thickness via "Lathing machine " (fig:15) for five size 20 mm , 70 mm , 120 mm and 170 mm. Accordingly, this group which have not any wrapping layer because it is "controls specimens"

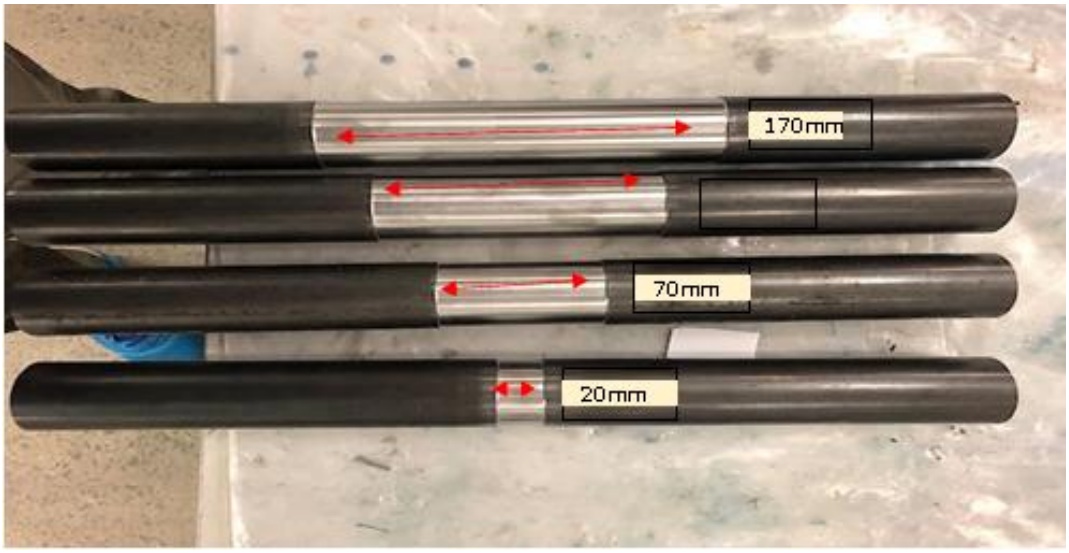

Figure 19: Group #3 which are without CFRP.

Group# 4: There were 2 specimens which cutting for 420mm of length. It has not any CFRP or cleaning before testing because this "Control simples".

Figure 20: Control specimens.

2. Types of equipment and test

In the Swinburne University Lab has this machine" MTS Landmark Servo hydraulic Test Systems "which applied all specimens for test "Monotonic OR Static Testing" which achieved test example; Tensile, compression and bend and stress relaxation. On the anther hand, it materialize ISO 6892 and ASTM E8,E9.E21.

Resource: COMAPNY, M. (2019). [online] Mts.com. Available at: https://www.mts.com/cs/groups/public/documents/library/dev_004324.pdf [Accessed 18 May 2019].

Figure 21: MTS Landmark Servo hydraulic Test Systems.

This machine which adjusted on 6 to 10 min/mm and the high displacement was 80mm. All thisinformation which added via technical thine. However, we fixed laser to calculated displacement which may be correct any mistake happens during applied load.

In addition, We staring with **Group#4** which called “control simples”. Fig: 21 which show us simple on machine under load:

Figure 23: MTS Landmark Servo hydraulic Test Systems for control specimen.

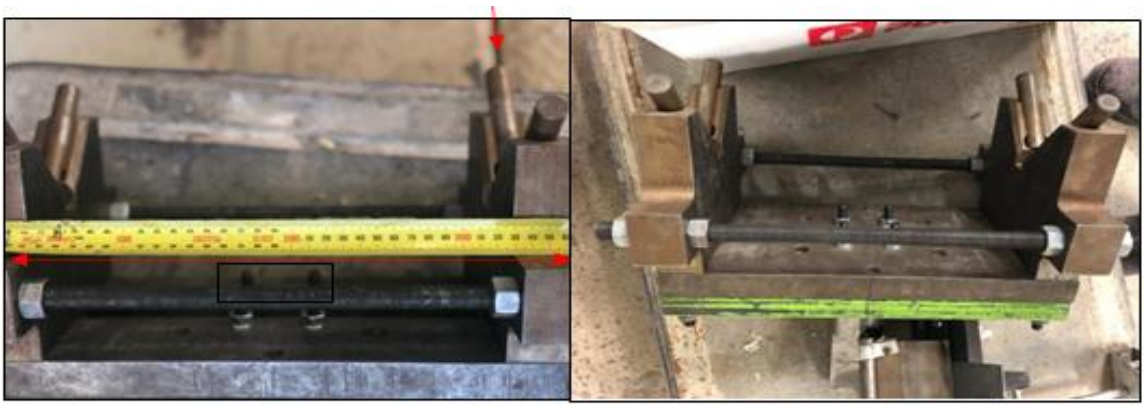

Figure 22: Support frame "base" 360mm from edge.

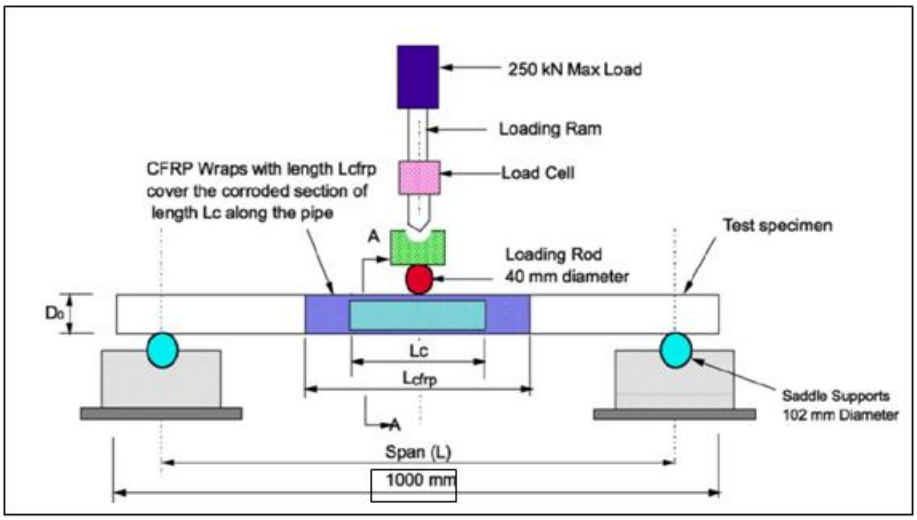

Figure 24: Drawing MTA machine with basement specimen.

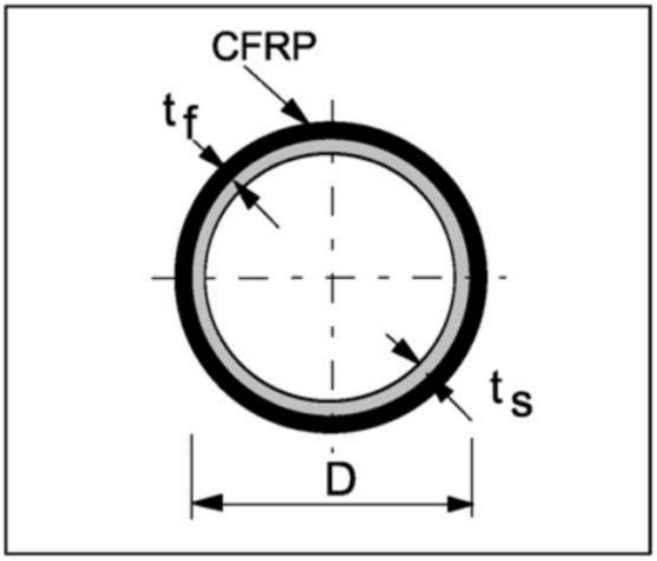

Figure 25: Section for CHS pipe tube with CFRP.

3. RESULTS AND DISCUSSION

The experiment established the candid relationship between the lateral displacements maximum which is 80 mm while the overall transverse static load in line with the force for the tested specimen. The tabulated results obtained from the analysis mainly indicated shown in the table below:

- **Group#1**

It is a clear for us, the last 3 specimens which have same Axial force and it is high ductility. However, the first simple "50 mm" which debonding CFRP.

Specimens ID	Axial load	Axial displacement	Laser reading
Group# 1:			
50 mm	12.52	79.98	85.26
100mm	13.425	80	82.400
150mm	13.5	79.99	81.64
200mm	13.816	67.6	69
250mm	13.533	75.6	77.47

Figure 26: Group#1 under test load and displacement.

Figure 27: Group#1 after applied test.

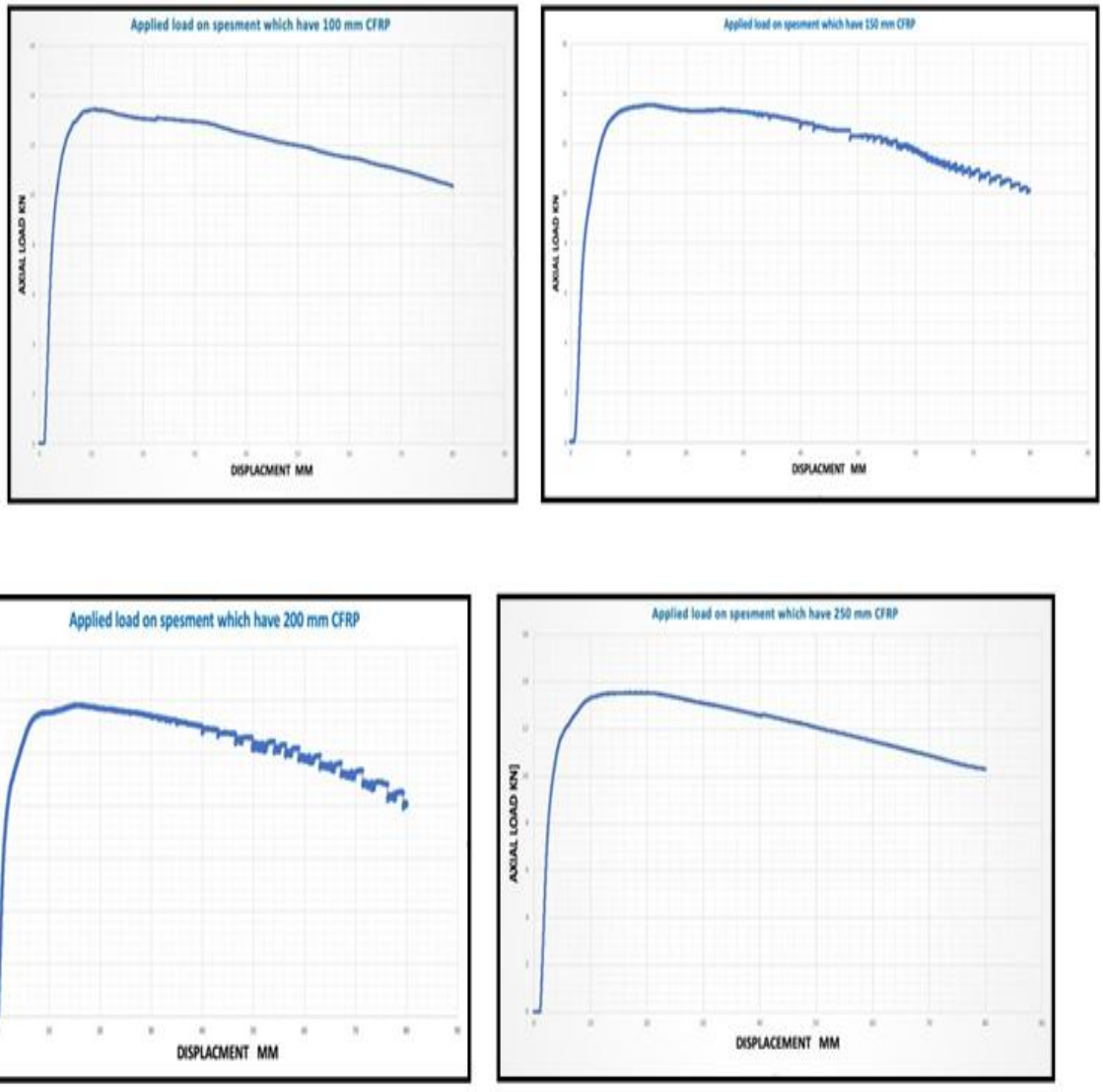

Figure 28: Graph for all specimens (Axial load VS Displacement*).*

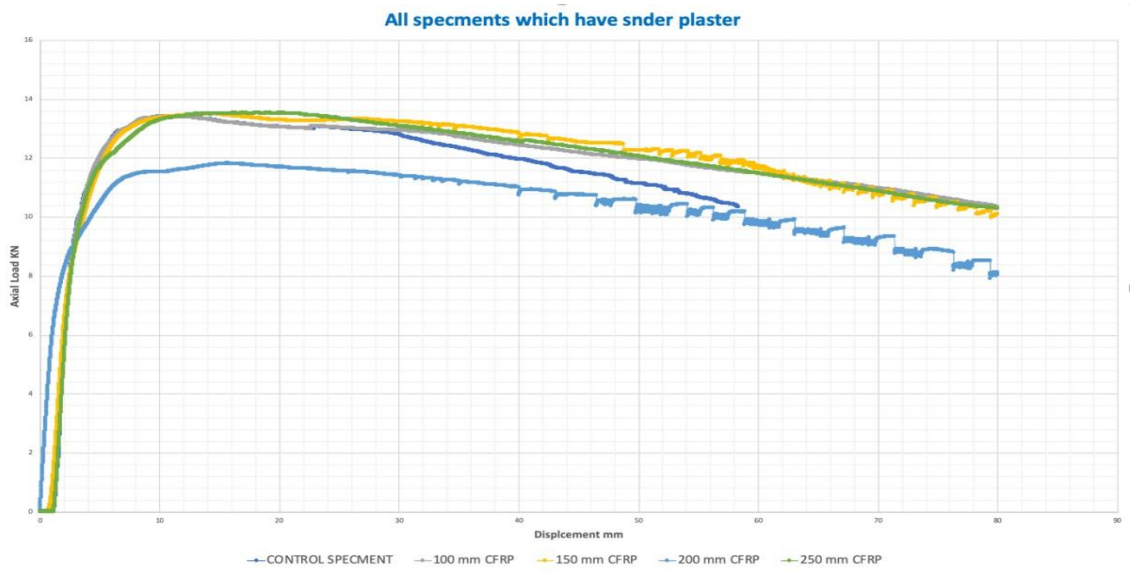

Figure 29: Figure 25: Graph for all specimens (Axial load VS Displacement).

It is clear from graph that controls simple which have lowest resistance Axial load. However, it has longest ductility. On the other hand, the length 100mm,150mm and 250 mm have similar behaver but simple 200 mm length which has lowest ductility. Furthermore, the control simple which has high performance in begin but it failed at 60 mm.

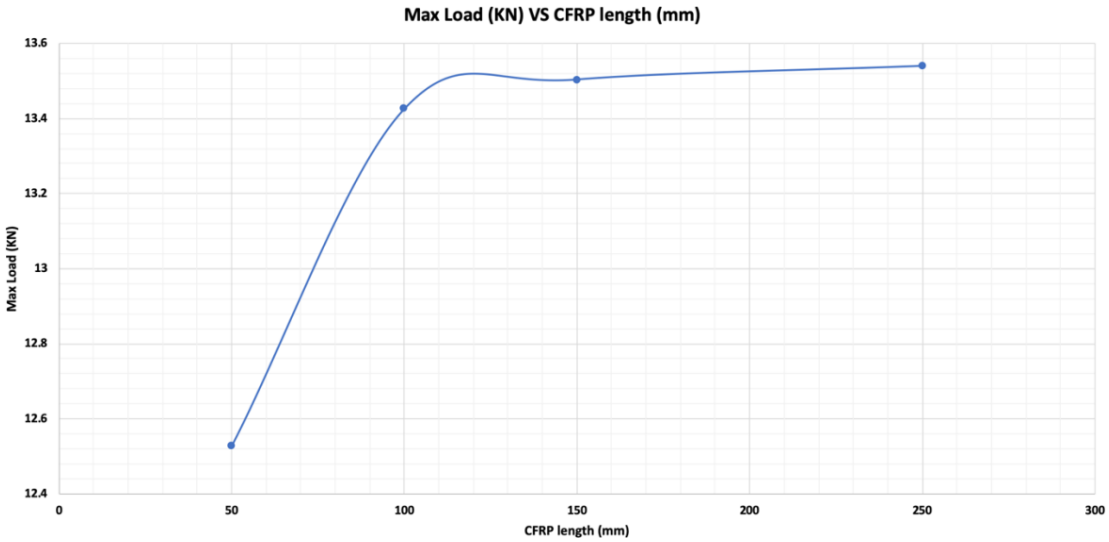

Figure 30: Max Load (KN) VS CFRP length (mm).

From above (fig:27): It clear that length of CFRP increasing resentencing load but at 150 mm and 250mm, it increase slightly.

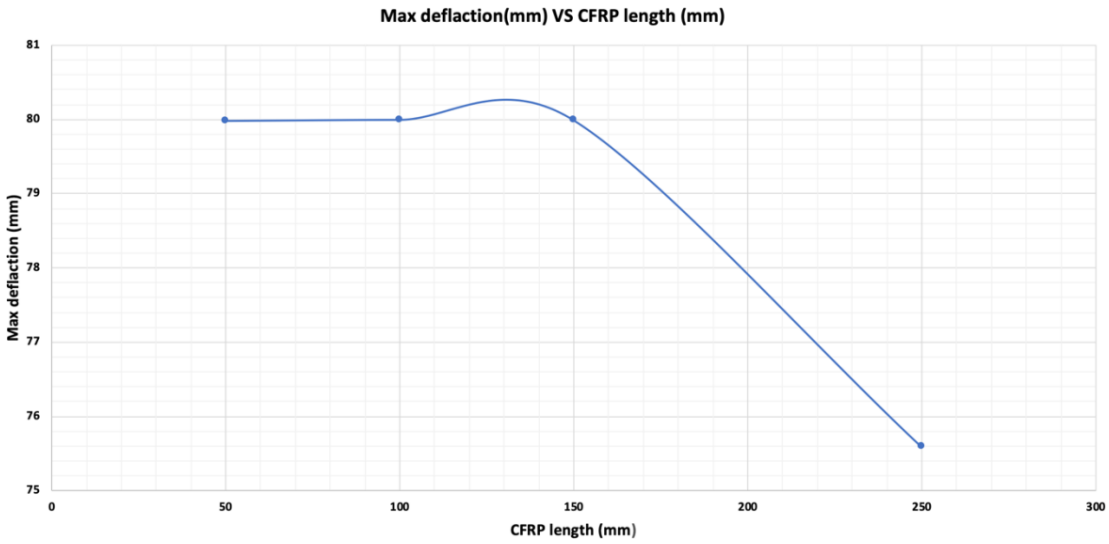

Figure 31: Max deflection (mm) VS CFRP length (mm).

To regards, the graph above, there was lowest deflection at 250 mm. Thus, CFRP length inversely proportional with deflection.

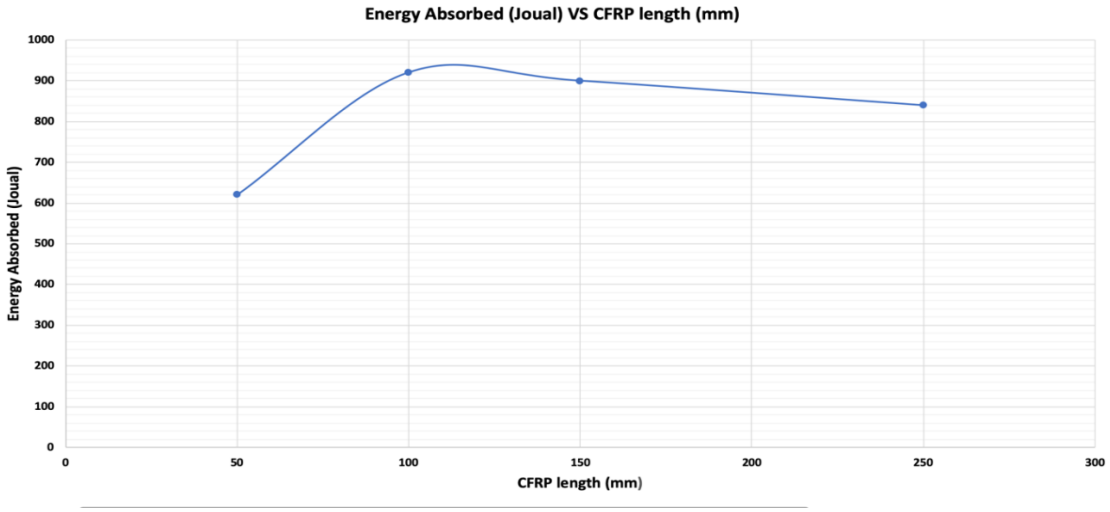

Figure 32: Energy Absorbed (Joual) VS CFRP length (mm).

The energy absorbed at long length of CFRP more than a short length of CFRP as showing above. However, the energy absorbed between 150mm and 250mm is little. This indicter that the CFRP is ineffective when become length longer the critical length.

- **Group#2**

It is a clear for us, the most specimens which have lower Axial load if we compare with Group#1. Moreover, the two simple 50 mm and 100 mm have deboning of CFRP.

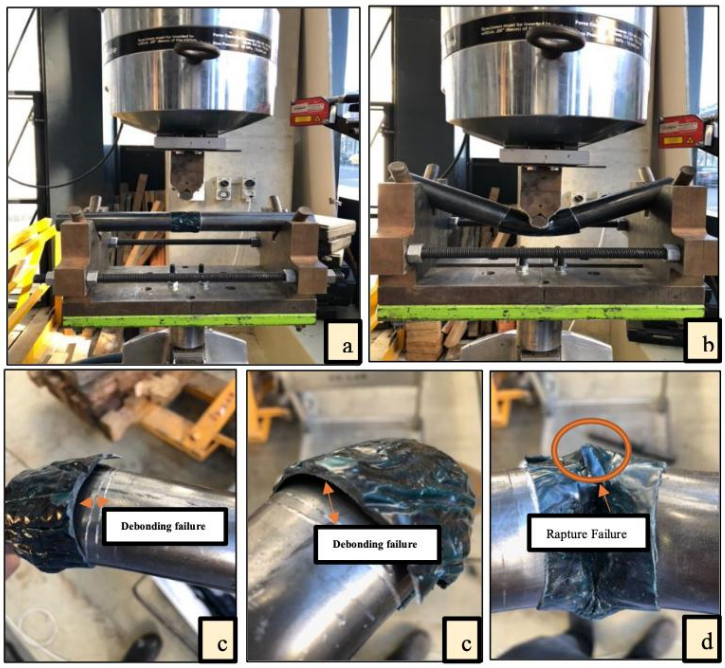

Figure 33: Photos for 50mm width of CFRP which cover 20 mm width which is reducing thinness 0.6 mm. a) under static load for 50mm, b) under static load for simple 50mm, c) demanding layers of CFRP for 50mm and 100mm, d) Failure mode.

While, the simple which cover 150mm and 200 mm of CFRP. It has not debonding showing However, it has lowest Axial load about 12% of 50mm and 100mm.

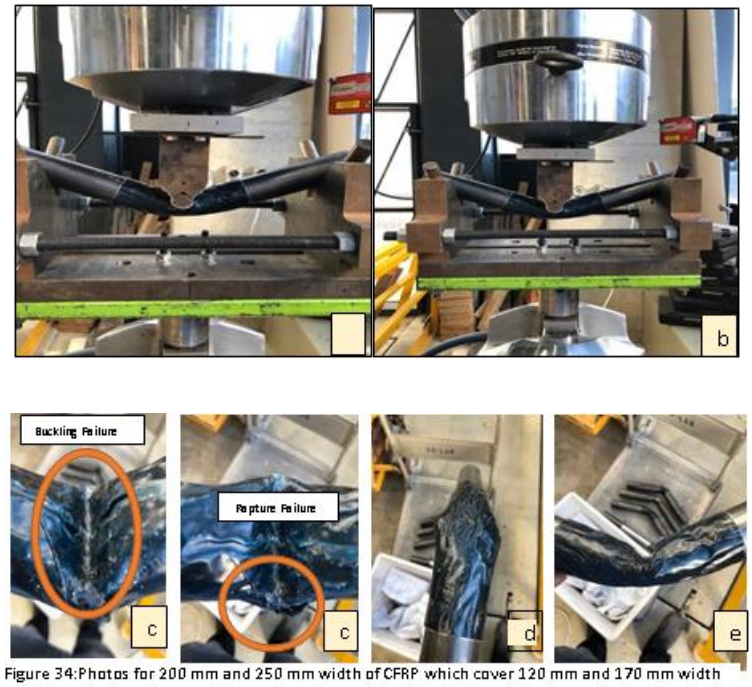

Figure 34:Photos for 200 mm and 250 mm width of CFRP which cover 120 mm and 170 mm width which is reducing thinness 0.6 mm. a) under static load for 200mm, b) under static load for simple 250mm, c) demanding layers of CFRP for 200 mm and 250 mm, d and e) no debonding on bottom

Figure 35: photo for all specimens after testing.

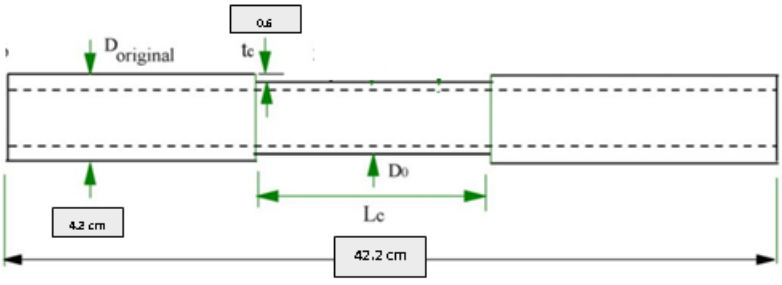

Figure 36: Section of specimen which have lathing.

Specimens ID	Axial load	Axial displacement	Laser reading
Group# 2:			
20 mm lathing (width) with 50 mm CFRP	9.47	67.34	67.85
70 mm lathing (width) with 100 CFRP	9.38	79.98	82.2477
120 mm lathing (width) without CFRP	7.935	74.488	76.33
170 mm lathing (width) with CFRP	7.815	76	78.33

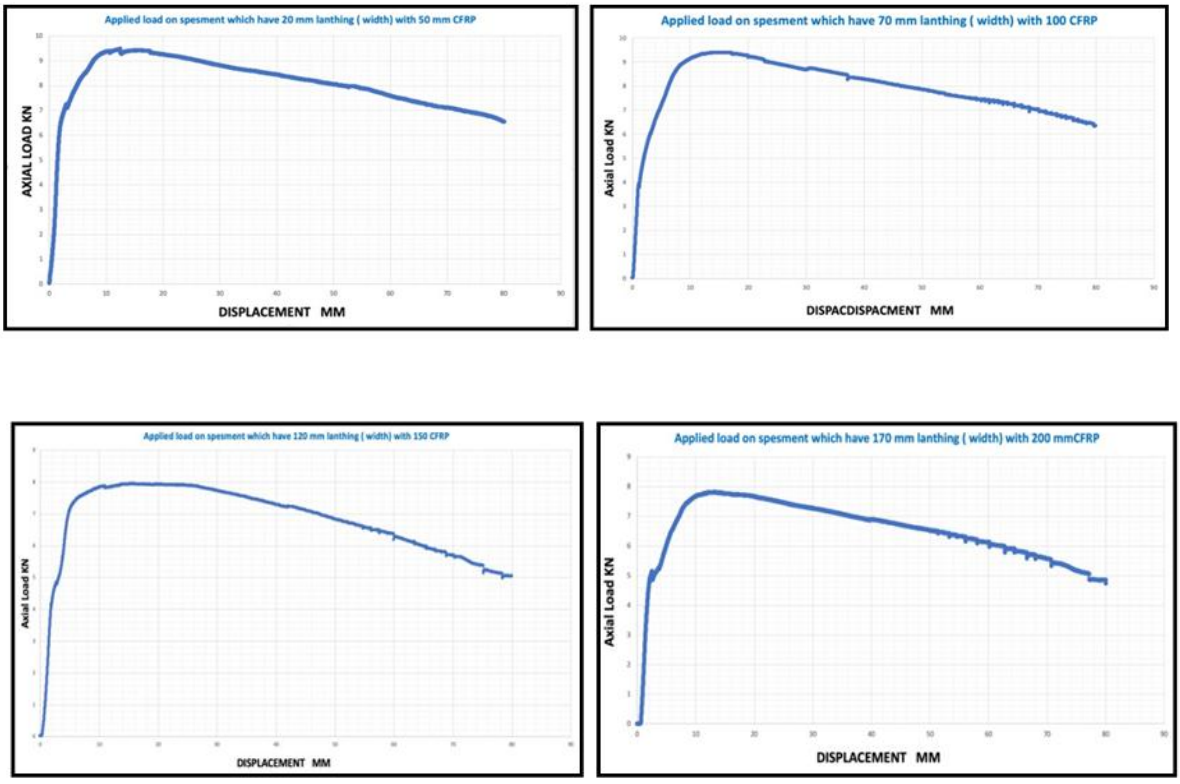

Figure 37: Test#2 for specimens which are reducing 0.6 mm for width 20,70,120 and 170 mm.

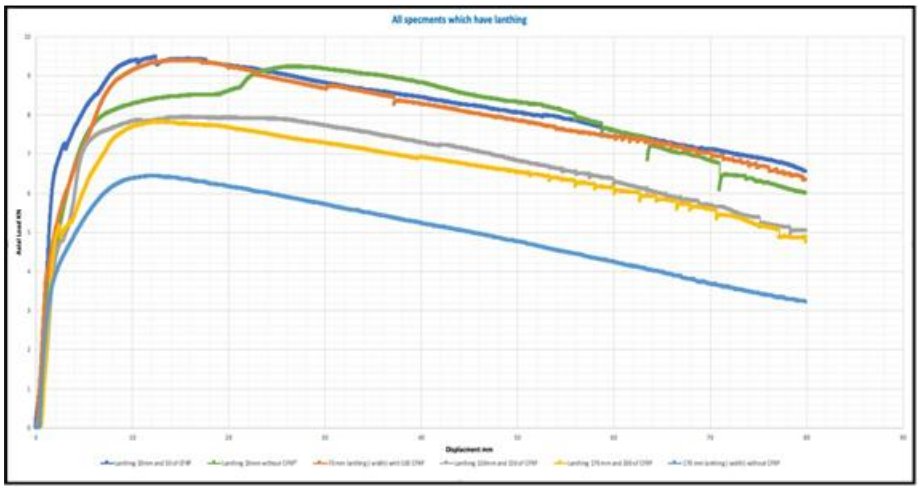

Figure 38: All specimens which have 20mm, 70mm, 120mm and 170 mm.

It is clear from the graph that 170mm lathing which warping 200 of CFRP which have lowest resistance but it has more ductility. On the other hand, the simple which has lather 20mm high and 50 mm of CFRP higher Axial load if we compare with other specimens. During pierid 25 mm to 55 mm, the highest load carry by 20 mm without lathing.

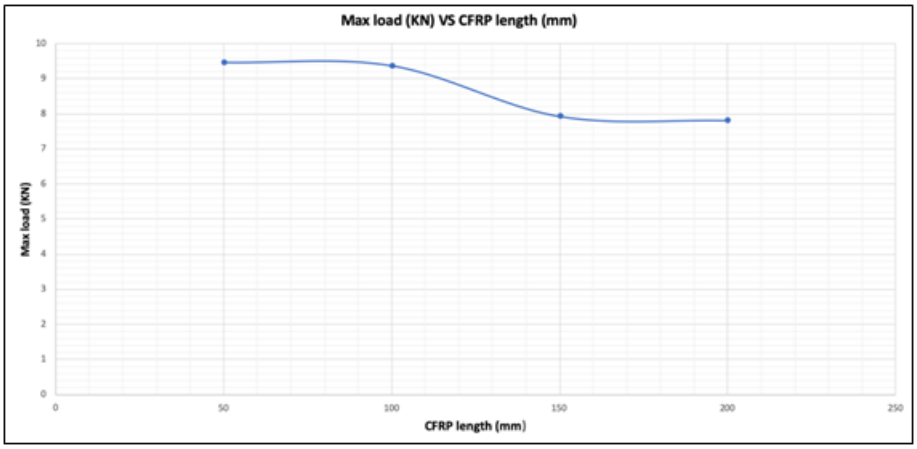

Figure 39: Max load (KN) VS CFRP length (mm).

From fig:37; The lengths 50 mm and 100 mm of CFRP have highest resisting axial load while 150 mm and 200 of CFRP have lowset axial load. To inference that the lathing is inversely proportional to resistance load.

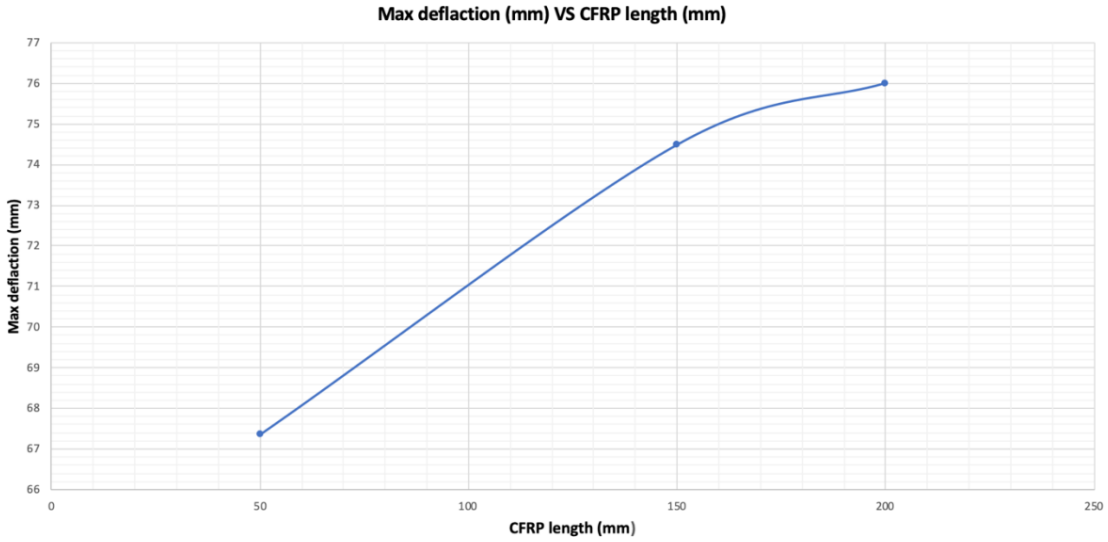

Figure 40: Max deflection (mm) VS CFRP length (mm).

To regards, the graph above, there was lowest deflection at 50 mm while highest at 200. We can read this graph that The CFRP can Increasing stuffiness with lathing.

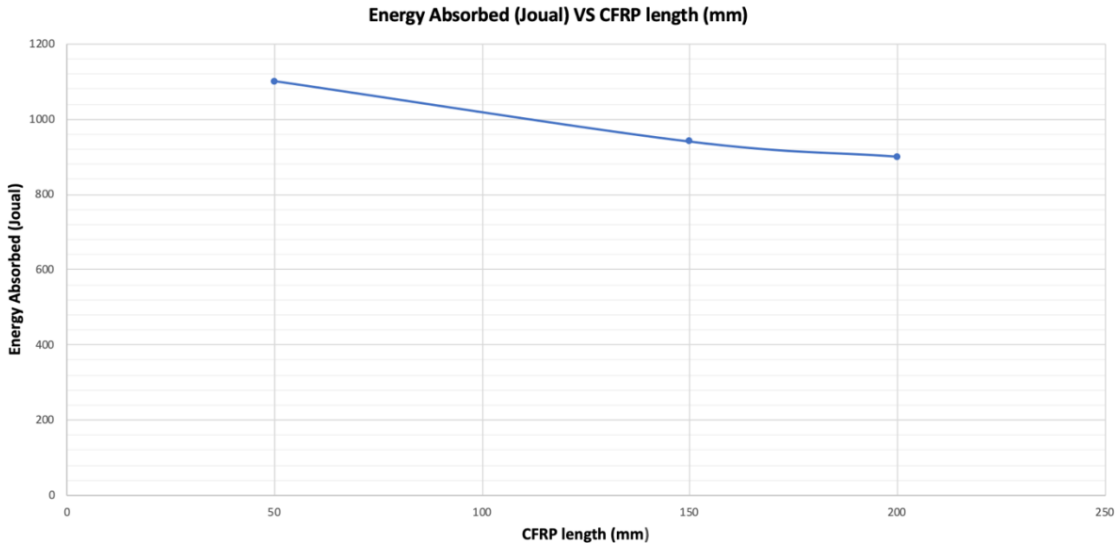

Figure 41: Energy Absorbed (Joual) VS CFRP length (mm).

The energy absorbed(fig:39) for length 50 mm of CFRP was big value if we compared with 150 mm and 200 mm of CFRP which have lowest energy absorbed result of reducing dimeter 0.6mm.

- **Group#3**

The test which need to confirmed result with simple which have not any change of body tube. We applied this test for two specimens which are without CFRP. Furthermore, we called this simple is "Control A and Control B".

Figure 42: Control specimen under static load.

To regard, the previous test for Group#1. It is common for us that, The specimens which have CFRP more resistance of control same which was Axial load 10.5 KN. Moreover,

the displacement higher than group #1.

Specimens ID	Axial load	Axial displacement	Laser reading
Group# 3:			
Control#1	11.22	81.95	81.97
Control#2	11.5	81.45	81.6

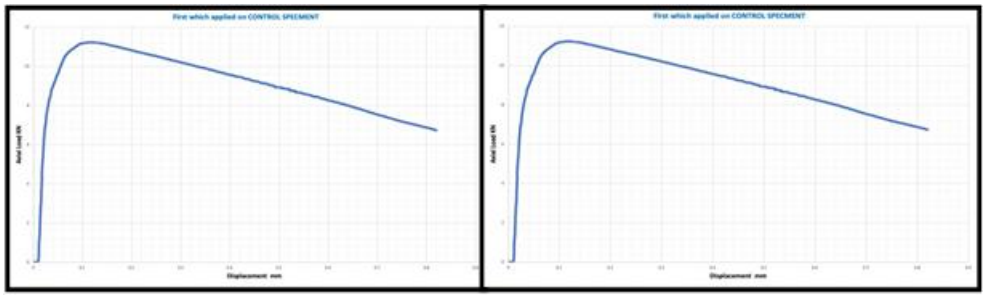

Figure 43: Figure 46: Two control specimens which have 50 mm.

- **Group#4**

This group similar last group#3 but we reduced the thickness about 0.6 of total dimeter. We have two simple, first one which reduced 0.6 mm for 20mm and 170 mm.

Figure 44: Lathing for 20 mm and 170 mm.

When applied load for these simple. There was different amount to resisters. The simple which have long lathing (170 mm) resistance less than simple which has short lathing.

Specimens ID	Axial load	Axial displacement	Laser reading
Group# 3:			
Control lathing#20 mm	9.22	63.30	64.76
Control lathing#170 mm	6.428	40.99	42.12

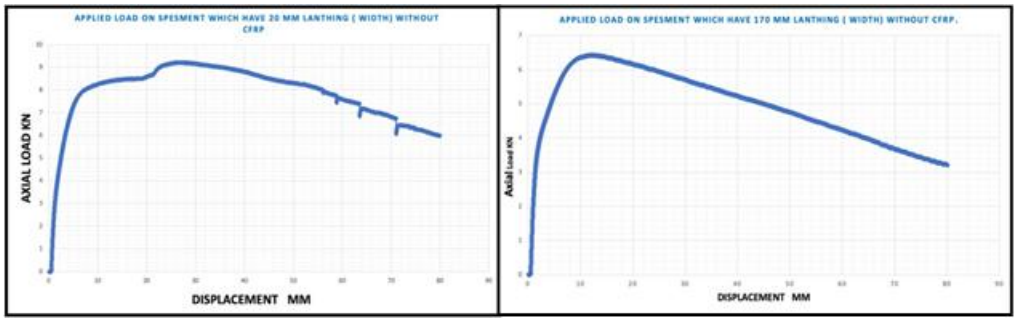

Figure 45: Two control specimens which have 20 mm and 170 mm.

To summarize all group as table down

Specimens ID	Axial load	Axial displacement	Laser reading	Persntage%
Group# 1:				
50 mm	12.5	80.0	85.3	10.5
100mm	13.4	80.0	82.4	16.6
150mm	13.5	80.0	81.6	17.0
200mm	11.8	67.6	69.0	5.2
250mm	13.5	75.6	77.5	17.2
Group# 2:				
20 mm lathing (width) with 50 mm CFRP	9.5	67.3	67.9	2.6
70 mm lathing (width) with 100 CFRP	9.4	80.0	82.2	
120 mm lathing (width) with150 mm of CFRP	7.9	74.5	76.3	
170 mm lathing (width) with 200 mm of CFRP	7.8	76.0	78.3	17.7
Group# 3:				
Control#1	11.2	82.0	82.0	17.8
Control#2	11.5	81.5	81.6	44.1
Group# 4:				
Control lathing#20 mm	9.2	63.3	64.8	19.8
Control lathing#170 mm	6.4	41.0	42.1	42.7

Table 4: Summary for all specimens and comparing.

From table 4, there were many of variation between Axial load which resisted by CFRP: The control speciment"group3" which compared with all specimens in group #1. The large resisting was 17.2% with 250 mm of CFRP. On the other hand , the control simple which lather 170 mm of whole length less than 170 mmm with 200 of CFRP axial load resist About 17.7%

a. Summary

There are different major and vital outcomes which one can draw from this research project. The analysis of the various components mainly summarized as indicated below.

1. There was initial peak variation on the specimen impact force and this was evident as result of the different contact surfaces applied in the process in line with wrapped hardness. Notably, there results for the residual forces and static load recorded for

this experiment were vividly similar across the board. There was remarkable static load in line with the resistance capacity and this was recorded by the externally and bonded CFRP sheet. It vividly indicated the reduction in the lateral displacement with a tune of at least 10.5% as compared to the bare specimen (Grouo#2). Furthermore, the group# 2 which rise up strength until 17.74%. On other the hand, it is a possible for us to notes that the CFRP achieved increasing of stuffiness pipe tube.

2. Notably, there are immense effects and applied load which is the CFRP orientations tend to have in the overall performance of the structure in line with the strengthened members. On the other hand, the it was reported that the CFRP were unable to minimize the local related deformations whereas they were excellent in curbing and controlling the global deformation.
3. The overall effective CFRP bond lengths mainly estimated to range from the 50% to 70%of the whole wrapping length. Also, there was reporting on the deflection of the specimen resistance capacity and this indicated the reduction of the bond length. However, the analysis was reported to have been similar to the overall strengthened length of the specimen.
4. All the specimens utilized in the experimental analysis depicted local and inward deformation. The norm was not only evident at the global deformation but also at the compression face. The additional norm also reported at the contact location and the tension face. Moreover, there were reports on the CFRP matrix and debonding and this lead to the reporting of the cracking failures which was noticed among the wrapped members. Conversely, there minimal cases reported for the end failures in line with the CFRP and GFRP. Thus, the analysis indicated the vast static mainly concentrated at the makeable mid-span regions of the specimen. There was also the dissipation of the impact energy via the global deformation of the different specimen. The dissipated energy resulted from both the strengthened as well as bare specimens due to the global deformation. The hastening of the strengthened members via the incorporation of the bending stiffness mainly aims at increasing the elastic rebound energies as compared to those of the bare members.
5. During the test, we can notes that:

- There was a relationship between resisters load axial force for 3 last simple of Group#1. Moreover, the simple which have long Wrapping, it's more ductility before failures. For example: the simple which warped 250mm more ductal than the simple which warped 150 mm.

- Most faultier happened on local deformation while the global deformation is stilling non deformation.
- It is a possible for us to apply more layer which may be increasing resisting load applied.

a. CONCLUSION

The reported indicates the performance recorded for the evaluation of the FRP strengthened CHS steel members. The elements were subjected to the transverse static load and the various results appraised and documented. The results gathered from the experimental analysis indicated the importance of incorporating the FRP wrapping in the CHS steel forms. The inclusion helps in enhancing both the members' capacities as well as the sections of the various tubular specimens when they subjected the lateral impacts. Also, there different buckling behaviours as well as domains which one must consider and evaluate when handling the structural and civil engineering works. Further to this, there the location and the optimum sizes of the FRP sheets which one requires to prevent the shortcomings associated with the elephant's foot buckling. The analysis for such considerations mainly considered viable in the pressurized cylindrical shell which has been depicted and identified in this research. The literature study also depicted the compressive examination of the CFRP applications and its effects on the structural CHS gap promotion in the K-joints. The analysis appraised the finite and experimental analysis regarding the different variables. The variables were examined in line with their static load on the ultimate joint bearing capacity.

Likewise, central areas of CFRP composite were situated at the hole between supports and along crossing point line among harmony and prop under strain, which gave further advancement system to the proposed CFRP establishment strategy. It has been demonstrated that the reinforcing impact of the FRP is touchy to its thickness, tallness and area, and ideal qualities for the total of what three have been distinguished for the full scope of pivotal burdens and interior weights. It has been appeared little varieties from the ideal qualities lead to altogether diminished conditions. The affectability of the clasping burden to the thickness and tallness of the FRP band has been appeared to be critical, while the separation over the base at which the FRP band should begin is considerably less. The observational equations for ideal reinforcing are adequately broad to be embraced in down to earth plans.

Finally, this paper simulated multi cases of CHS as lathing and sand plaster surface. The most resulting indication that there is many of benefit to using CFRP to a stronger member of the structure. This reported result of much time which has been spender in Lab at Swinburne University during 12 Weeks. This period study Considered very short to exams many of CHS and CFRP with different layers but I will complete tests in Ph.D. in future near.

ACKNOWLEDGEMENT

We would like to across our thankfulness and assessment to our supervisor Dr. Alaa Alamosa which is a member in Faculty of Engineering and Technology in the Swinburne University of Technology for encouraging and support us during this Project research which advise us throughout the whole project research.

On the other hand, I would like to thanks the candidate for Ph.D. Mr.Ammar bed which worked with us during lab experiment and giving the right advice and explained "how to use types of equipment. Moreover, he supervised an experiment test and he rechecks resulting and process which following up. Mr. Bed member of Faculty of Engineering and Technology.

Finally, I would like to up thank all member of labs which were very friendly to proof advising and materials.

DECLARATION

We would like to confirm that:

This research never had related any someone word, or copies word reference except which reference has been made in the quotation.

We confirm that this paper which has first submission in Swinburne University system.

III. REFERENCES

1. Abu-Sena, A. B. B. *et al*, 'Behavior of hollow steel sections strengthened with CFRP', *Construction and Building Materials*. Elsevier Ltd, 2019; 205: 306–320.
2. Al-saadi, A. U., Aravinthan, T. and Lokuge, W. 'Structural applications of fibre reinforced polymer (FRP) composite tubes: A review of columns members', *Composite Structures*. Elsevier, 2018; 204(May): 513–524.

3. Alam, M.I., Fawzia, S., Zhao, X.L. and Remennikov, A.M,' Experimental study on FRP- strengthened steel tubular members under lateral impact', *Journal of Composites for Construction*, 2017; *21(*5).
4. Alam, M.I., Fawzia, S., Zhao, X.L., Remennikov, A.M., Bambach, M.R. and Elchalakani, M.,' Performance and dynamic behaviour of FRP strengthened CFST members subjected to lateral impact', *Engineering Structures*, 2017; *147*: 160-176.
5. Batikha, M., Chen, J.F. and Rotter, J.M., Fibre reinforced polymer for strengthening cylindrical metal shells against elephant's foot buckling: An elasto-plastic analysis', *Advances in Structural Engineering*, 2018; *21(*16): 2483-2498.
6. Cascardi, A., Micelli, F. and Aiello, M.A., Unified model for hollow columns externally confined by FRP', *Engineering Structures*, 2016; *111*: 119-130.
7. Chahkand, N.A., Jumaat, M.Z., Sulong, N.R., Zhao, X.L. and Mohammadizadeh, M.R., Experimental and theoretical investigation on torsional behaviour of CFRP strengthened square hollow steel section', *Thin-Walled Structures*, 2013; *68*: 135-140.
8. Chellapandian, M., Prakash, S.S. and Sharma, A., Experimental and finite element studies on the flexural behavior of reinforced concrete elements strengthened with hybrid FRP technique', *Composite Structures*, 2019; *208*: 466-478.
9. Chen, T., Wang, X. and Qi, M., Fatigue improvements of cracked rectangular hollow section steel beams strengthened with CFRP plates', *Thin-Walled Structures*, 2018; *122*: 371- 377.
10. Chen, Y., Chen, X. and Wang, C., Web crippling of galvanized steel tube strengthened by CFRP sheets', *Composites Part B: Engineering*, 2016; *84*: 200-210.
11. Djerrad, A., Fan, F., Zhi, X. and Wu, Q., Experimental and FEM analysis of AFRP strengthened short and long steel tube under axial compression', *Thin-Walled Structures*, 2019; *139*: 9-23.
12. Dlugosch, M., Fritsch, J., Lukaszewicz, D. and Hiermaier, S., Experimental investigation and evaluation of numerical modeling approaches for hybrid-FRP-steel sections under impact loading for the application in automotive crash-structures', *Composite Structures*, 2017; *174*: 338-347.
13. Dong, J.F., Wang, Q.Y. and Guan, Z.W., Structural behaviour of recycled aggregate concrete filled steel tube columns strengthened by CFRP', *Engineering Structures*, 2013; *48*: 532-542.
14. El-Sayed, K.M., Debaiky, A.S., Khalil, N.N. and El-Shenawy, I.M., Improving buckling

resistance of hollow structural steel columns strengthened with polymer-mortar', *Thin-Walled Structures*, 2019; *137*: 515-526.

15. Feng, P., Hu, L., Qian, P. and Ye, L., Buckling behavior of CFRP-aluminum alloy hybrid tubes in axial compression', *Engineering Structures*, 2017; *132*: 624-636.
16. Feng, P., Hu, L., Zhang, Y. and Ye, L., Behavior analysis of FRP tube/filling strengthened steel members under axial compression', *Thin-Walled Structures*, 2019: *134*: 475-490.
17. Feng, P., Hu, L., Zhao, X.L., Cheng, L. and Xu, S., Study on thermal effects on fatigue behavior of cracked steel plates strengthened by CFRP sheets', *Thin-Walled Structures*, 2014; *82*: 311-320.
18. Fu, Y., Tong, L., He, L. and Zhao, X.L., Experimental and numerical investigation on behavior of CFRP-strengthened circular hollow section gap K-joints', *Thin-Walled Structures*, 2016; *102*: 80-97.
19. Gambarelli, S., Nisticò, N. and Ožbolt, J., Numerical analysis of compressed concrete columns confined with CFRP: Microplane-based approach', *Composites Part B: Engineering*, 2014; *67*: 303-312.
20. Gao, X.Y., Balendra, T. and Koh, C.G., Buckling strength of slender circular tubular steel braces strengthened by CFRP', *Engineering structures*, 2013; *46*: 547-556.
21. Ghaemdoust, M.R., Narmashiri, K. and Yousefi, O., Structural behaviors of deficient steel SHS short columns strengthened using CFRP', *Construction and Building Materials*, 2016; *126*: 1002-1011.
22. Haedir, J. and Zhao, X.L., Design of CFRP-strengthened steel CHS tubular beams', *Journal of Constructional Steel Research*, 2012; 72: 203-218.
23. Haedir, J., Bambach, M.R., Zhao, X.L. and Grzebieta, R.H., Strength of circular hollow sections (CHS) tubular beams externally reinforced by carbon FRP sheets in pure bending', *Thin-walled structures*, 2009; 47*(*10): 1136-1147.
24. Hu, H. and Seracino, R., Analytical model for FRP-and-steel-confined circular concrete columns in compression', *Journal of Composites for Construction*, 2013; 18(3): A4013012.
25. Hu, L., Feng, P. and Zhao, X.L., Fatigue design of CFRP strengthened steel members', *Thin-Walled Structures*, 2017; 119: 482-498.
26. Islam, S.Z. and Young, B., Ferritic stainless steel tubular members strengthened with high modulus CFRP plate subjected to web crippling', *Journal of Constructional Steel Research*, 2012; 77: 107-118.

27. Islam, S.Z. and Young, B., FRP strengthening of lean duplex stainless steel hollow sections subjected to web crippling', *Thin-Walled Structures*, 2014; *85*: 183-200.
28. Kabir, M.H., Fawzia, S. and Chan, T.H., Durability of CFRP strengthened circular hollow steel members under cold weather: Experimental and numerical investigation', *Construction and Building Materials,* 2016; 123: 372-383.
29. Kabir, M.H., Fawzia, S., Chan, T.H. and Badawi, M., Durability of CFRP strengthened steel circular hollow section member exposed to sea water', *Construction and Building Materials*, 2016; *118*: 216-225.
30. Kabir, M.H., Fawzia, S., Chan, T.H. and Gamage, J.C.P.H., Durability performance of carbon fibre-reinforced polymer strengthened circular hollow steel members under cold weather', *Australian Journal of Structural Engineering*, 2014; *15(*4): 377-392.
31. Kabir, M.H., Fawzia, S., Chan, T.H.T. and Badawi, M., Numerical studies on CFRP strengthened steel circular members under marine environment', *Materials and Structures*, 2016; *49(*10): 4201-4216.
32. Kabir, M.H., Fawzia, S., Chan, T.H.T., Gamage, J.C.P.H. and Bai, J.B., Experimental and numerical investigation of the behaviour of CFRP strengthened CHS beams subjected to bending', *Engineering Structures*, 2016; 113: 160-173.
33. Kadhim, M.M., Wu, Z. and Cunningham, L.S., Numerical study of full-scale CFRP strengthened open-section steel columns under transverse impact', *Thin-Walled Structures*, 2019; 140: 99-113.
34. Kalavagunta, S., Naganathan, S. and Mustapha, K.N., Axially loaded steel columns strengthened with CFRP', *Jordan Journal of Civil Engineering*, 2014; *159:* 3175: 1-12.
35. Katrizadeh, E. and Narmashiri, K., Experimental study on failure modes of MF-CFRP strengthened steel beams', *Journal of Constructional Steel Research*, 2019; *158*: 120-129.
36. Keykha, A.H., 3D finite element analysis of deficient hollow steel beams strengthened using CFRP composite under torsional load', *Composites: Mechanics, Computations, Applications: An International Journal*, 2017; *8(*4).
37. Keykha, A.H., Structural performance evaluation of deficient steel members strengthened using CFRP under combined tensile, torsional and lateral loading', *Journal of Building Engineering*, 2019; 100746.
38. Keykha, A.H., Nekooei, M. and Rahgozar, R., Analysis and strengthening of SHS steel columns using CFRP composite materials', *Composites: Mechanics, Computations, Applications: An International Journal*, 2016; *7(*4).

39. Lesani, M., Bahaari, M.R. and Shokrieh, M.M., 'Numerical investigation of FRP-strengthened tubular T-joints under axial compressive loads', *Composite structures*, 2013; 100: 71-78.
40. Lesani, M., Bahaari, M.R. and Shokrieh, M.M., Experimental investigation of FRP-strengthened tubular T-joints under axial compressive loads', *Construction and building materials*, 2014; 53: 243-252.
41. Lesani, M., Bahaari, M.R. and Shokrieh, M.M., FRP wrapping for the rehabilitation of Circular Hollow Section (CHS) tubular steel connections', *Thin-Walled Structures*, 2015; 90: 216-234.
42. Li, S.Q., Chen, J.F., Bisby, L.A., Hu, Y.M. and Teng, J.G., Strain efficiency of FRP jackets in FRP-confined concrete-filled circular steel tubes', *International Journal of Structural Stability and Dynamics*, 2012; *12(*1): 75-94.
43. Park, J.W., Yeom, H.J. and Yoo, J.H., Axial loading tests and FEM analysis of slender square hollow section (SHS) stub columns strengthened with carbon fiber reinforced polymers', *International Journal of Steel Structures*, 2013; *13(*4): 731-743.
44. Parvin, A. and Brighton, D., FRP composites strengthening of concrete columns under various loading conditions', *Polymers*, 2014; *6(*4): 1040-1056.
45. Selvaraj, S. and Madhavan, M., 'CFRP strengthened steel beams: Improvement in failure modes and performance analysis', In *Structures*, 2017; 12: 120-131.
46. Shakir, A.S., Guan, Z.W. and Jones, S.W., Lateral impact response of the concrete filled steel tube columns with and without CFRP strengthening,' *Engineering structures*, 2016; 116: 148-162.
47. Shen, K., Wan, S., Mo, Y.L. and Jiang, Z., Theoretical analysis on full torsional behavior of RC beams strengthened with FRP materials', *Composite Structures*, 2018; 183: 347-357.
48. Shen, Q., Wang, J., Wang, J. and Ding, Z., Axial compressive performance of circular CFST columns partially wrapped by carbon FRP', *Journal of Constructional Steel Research*, 2019; 155: 90-106.
49. Elchalakani, M. Rehabilitation of corroded steel CHS under combined bending and bearing using CFRP', *Journal of Constructional Steel Research*, 2016; 125: 26-42.